Author's response for amt-2017-236

Daniel Zawada et al.

November 24, 2017

We would like to thank the editor for handling the manuscript and the reviewers for their helpful comments. What follows is a point by point response to each of the reviewers suggestions as well as a marked up version of the changes in the revised manuscript.

We would like to thank the referee for their helpful comments and suggestions. Included below is each of the referee's comments (italics) followed by our reply.

Responses to Referee 1 (Alexei Rozanov)

General Comments

Authors use outdated versions of OMPS Level 1 data (v2.0-2.4) although the new data version v2.5 is available already since May 2017. As version 2.5 already includes the pointing correction described in Sect. 3 of the manuscript this section would not be necessary any more if new Level 1 data was used.

Reply: It is true that a similar pointing correction has been included in the v2.5 L1G product, we have mentioned this in the revised manuscript. However we feel it is important to include the section as the manuscript serves as a description of our v1.0.2 retrieved ozone product which has already been used in several studies. We are planning on producing a new version of our ozone data product in the future based on the new L1G product but it is not feasible to include it here due to the computational burden of reprocessing the entire mission.

Pointing accuracy is mentioned as the main error source and the corrections in the order of 200-300 m seem to be considered by authors as important, oth- erwise one would rather skip Sect. 3. On the other hand, the authors do not hesitate to neglect the field of view of 1.5 km without making any considerations about the impact of this decision. As the field of view illumination is vertically inhomogeneous, I assume the neglect of field of view integration should have a similar effect as a misspointing. In this regard it is not quite clear why a very good agreement with MLS is still achieved and if the entire verification results might be accepted as trustable. To my opinion the evaluation must be repeated taking into account the field of view of the instrument.

Reply: We agree that neglecting the field of view has the potential to have an effect on the retrieval, however this is no trivial matter. The referee states that the field of view is 1.5 km, which is approximately true for a single pixel on the detector, but the provided level 1 product is gridded, bilinearly interpolated from four neighboring pixels. The actual field of view (both magnitude and shape) varies as a function of altitude and wavelength depending on where each pixel is, and this information is not publicly available. Furthermore, neglecting the instrumental field of view is a common assumption in many limb retrievals (including the operational NASA OMPS-LP retrieval and the OSIRIS retrieval, which this work builds upon) and we do not feel it is within the scope of this manuscript to perform a full study on this effect.

However, as stated in the manuscript we do intend to investigate this further in a future version of the retrieval. We expect that neglecting the field view has a vertical smoothing

effect, which is why we do not trust our predicted 1 km vertical resolution and instead estimate it as 1–2 km. Our preliminary tests have indicated that neglecting the field of view has the potential to introduce a 1–2 % high bias near 20–25 km. This is considerably less than the ∼7% error you could see with a 300 m pointing shift at high altitudes.

As an improvement of the retrieval quality by using a 2D retrieval is a key topic of the manuscript, synthetic retrievals as done in Sect. 5.1 need to be presented for the whole orbit. This is necessary to assess if smoothing out the small latitudinal variations by 2D retrieval as seen around 50° S in Fig. 8 is a general drawback of this approach or just an insignificant outlier. Furthermore, a similar study should be performed for another season with a vortex edge in the northern hemisphere. This will allow the reader to assess how the viewing geometry affects the relative performance of the 1D and 2D retrievals. Another important question is how the retrieval results depend on the ozone distribution used to initialize the radiative transfer model. This question has not been addressed in the manuscript at all.

Reply: We have changed the requested figure to show the entire orbit, and also added a second orbit using synthetic data with northern hemisphere ozone depletion. Internal tests have shown that the dependence on the profile used to initialize model is negligible ($\leq 1\%$), we have added a statement to the revised manuscript to this effect.

The retrieval description is too much general with a lot of details hidden from the reader. For example, no or only insufficient quantitative information is provided about the latitudinal grid, reference tangent height and regularization parameters γ in Eq. (2) and α in Eq. (3)). The authors state that the a priori state vector is set to zero but make no comments about the values used to initialize the radiative transfer model. Are they also zero at the first iteration? The valid altitude range of the retrieval in not clearly identified.

Reply: We agree that the retrieval description was too general in many places. In the revised manuscript the description of aspects of the retrieval such as the state vector are given directly for the retrieval as applied to OMPS-LP, rather than first for a theoretical retrieval. Many of these specific changes are outlined as replies to the referees other comments below.

The validation is not sufficient to demonstrate the overall performance of the algorithm. The monthly mean comparison plots similar to Fig. 10 must be provided for absolute values rather than for anomalies for several latitude bands (tropics, middle and high latitudes).

Reply: The provided comparisons are intended to demonstrate the validity of the technique and not be a full validation of the dataset, which we feel is beyond the scope of this manuscript. As stated in the manuscript the validation work presented is preliminary, and a full validation is planned for a future paper.

Detailed comments

Page 2, line 24 *"... $\gamma_i I$ might be included..." - please make a clear statement if this term is included in your retrieval or not, if yes, what is the starting value and a typical end value of γ_i?*

Reply: We have added the statement that a small $\gamma_i = 0.1\cdot$ the mean value of the diagonal of $\mathbf{K}_i^T \mathbf{S}_\epsilon^{-1} \mathbf{K}_i$ term is included to primarily aid with the stability of the inversion.

Sect. 2.2 *State vector is described insufficiently. Both altitude and latitude grids must be specified exactly providing the upper and lower limits as well as the sampling.*

Reply: This section has been rewritten, we have opted to immediately explain the state vector for ozone here rather than a generic state vector. The horizontal grid is not spaced in latitude, rather it is in angle along the orbital plane of OMPS-LP, we hope this is now clear. Upper and lower limits and sampling have been noted for both the vertical and horizontal components in the revised section.

Page 3, line 13 *"A consequence of the limb viewing geometry..." - this is not a general consequence of the limb viewing geometry as a scanning instrument can be operated to avoid this problem (e.g. SCIAMACHY). This is rather a con- sequence of the imaging technique (2D detector array) used in OMPS.*

Reply: We have changed the wording to "A consequence of the OMPS-LP viewing geometry"

Page 3, paragraph starting at line 16 *this is an unnecessary general discussion which do not provide any useful information. It is highly questionable if the method described by authors is really that general as no references are provided. Furthermore, possible griding issues vary with the observation method. For example the issues are completely different if a combination of measurements along and across the flying direction is used. I recommend to remove the paragraph and focus on the detailed description of the setup used in the retrieval rather than discussing any "general" approaches.*

Reply: We have removed this information.

Page 4, Sect. 2.3, starting from line 16 till the end of the section *to my opinion this text does not provide any useful information as for the retrieval/modeling description it is absolutely irrelevant whether the model performs the internal transformation of the coordinates or not. If you think it is important you need to describe it in much more details to give the reader*

understanding what is performed, how and for what reason, and which implications it can cause. Otherwise the text must be deleted as in its current form it is just confusing.

Reply: We have moved the figure and the text mentioning the mismatch between the instrument line of sight and the retrieval grid to the state vector section. We have also removed the text about the coordinate transformations as requested, and now simply state that the line of sight plane is projected onto the retrieval grid.

Page 5, lines 1-2 *"The sparsity of the Jacobian matrix can be improved..., as is done in Livesey et al. (2006)" - there are a lot of things which "can be done". The essential information is, however, if it "is done" in your retrieval or not. Please provide the numbers if it is done or clear statement that it is not done otherwise.*

Reply: We have added the statement "For our retrieval we limit each measurement to contribute to profiles within 10° of the tangent point.".

Page 5, lines 3-6 *This text does not contain any useful information. The matrices to be stored and inverted are already known from Eq. (2), their dimensions are already discussed in the first paragraph of the section, the fact if you solve the linear equation system using a solver for sparse or dense matrices is an absolutely minor technical information and a calculation of a memory space needed to store a 10000 × 10000 matrix is a very simple arithmetical exercise which is not relevant for a scientific paper.*

Reply: We agree that obviously calculating the storage requirements for a matrix is simple, but we do not agree that the information should be removed. One of the limiting factors for grid spacing, number of measurements used, etc., for a tomographic retrieval is computational. Other papers describing tomographic techniques such as Livesey et. al. 2006 and Ungermann et al. 2010 include similar types of information.

Ungermann, J., Kaufmann, M., Hoffmann, L., Preusse, P., Oelhaf, H., Friedl-Vallon, F., and Riese, M.: Towards a 3-D tomographic retrieval for the air-borne limb-imager GLORIA, Atmos. Meas. Tech., 3, 1647-1665, https://doi.org/10.5194/amt-3-1647-2010, 2010.

Livesey, N. J., Van Snyder, W., Read, W. G., and Wagner, P. A. (2006). Retrieval algorithms for the EOS Microwave limb sounder (MLS). IEEE transactions on geoscience and remote sensing, 44(5), 1144-1155.

Page 5, last paragraph *the paragraph is quite confusing. It not strictly defined what you understand as a "forward model run". In any case you have to simulate the radiance for every measured pixel, otherwise you just loose the information. Formally you can do just one "forward model run" and simulate everything. Thus, to understand this discussion, the reader has to know what is meant as a "run". Normally the forward model is run for*

each internal grid point, this might coincide with the location of the image or not. Surely a reduction of grid points reduces the computation time. So, actually, you just need to provide the information on the latitudinal grid and skip the remaining discussion.

Reply: We realize that this section was confusing for those who are not familiar with SASKTRAN. The point we were trying to convey is that the expensive part of the radiative transfer calculation is calculating the multiple scatter source function, J_{MS}, which is a function of space, atmospheric state, and time. Once we have J_{MS} the final line integrals take little effort. The potential for computational time saving here is that since the grid points are close to each other, we can calculate J_{MS} in a spatial region that covers multiple grid points. The problem is that each "run" of SASKTRAN is for a single instant of time, so doing that is not strictly valid because each measurement obviously does not occur at the same instant in the time. So in this section we attempted to describe the potential issues with assuming that ~ 5 measurements occur at the same instant of time (roughly 100 s), it has nothing to do with changing the number of grid points (the largest issue is that the sun is assumed to be in the same location over this 100 s). We have rewritten the majority of this section to try to make this more clear.

Page 6, line 1 *"10° cone" - commonly the term "cone" is used for a 3D object while you have a 2D approach. Please use a proper notation. Furthermore, it is unclear how this "cone" is defined, I suppose from the Earths center, but it should be clearly stated to avoid a confusion.*

Reply: We have added the statement that the cone's vertex is the Earth's center, however in this case we believe that cone is the correct term. While the retrieval is a 2D approach, as soon as the atmosphere is allowed to vary in a second dimension (other than SZA) the symmetry in the source function is broken and it becomes 5 dimensional (position, direction) rather than 4 dimensional (altitude, SZA, direction). The source function is solved within this three dimensional cone.

Page 6, line 3 *"Each image..." - do you mean that the solar zenith angle changes from image to image? It is actually obvious that the illumination and composition of the atmosphere changes from one location to anther. Why is it an issue?*

Reply: We hope that this is clearer now that we have rewritten this section. The issue is that each measurement happens at a different time, a single SASKTRAN-HR calculation is one instant of time, so modelling multiple measurements with one SASKTRAN-HR calculation involves an assumption.

Page 6, line 4 *"... internal atmosphere is specified as a plane" - I suppose you mean the*

meridional direction. It should be clearly stated to avoid a misinterpretation.

Reply: This has been changed to "as a plane in the along line of sight direction".

Sect. 2.5 *Actually I did not find anywhere a statement about the variable defining the along-orbit grid, is it latitude, solar zenith angle, of anything else?*

Reply: The grid is the angle within the orbital plane, we hope that in the revised manuscript this is clear.

Sect. 2.5 *The last paragraph does not contain any useful information as it is not discussed how the OSIRIS images are compiled and how the corresponding radiative transfer calculations are done. Surely the listed conditions are not an issue for 1D retrievals if each observation is processed independently. I recommend to remove the paragraph.*

Reply: We think the modified section and our previous answers has made this clear. The issues are very much the same for the OSIRIS 1D retrieval which assumes that each scan happens at one instant of time, rather than running a new radiative transfer calculation for each individual observation.

Sect. 2.6 *Remove the first two paragraphs of the section. These paragraphs pretend to provide an overview of the methods fail however to do that as the discussion is to sketchy. Furthermore, this information is not needed for the discussion below.*

Reply: We have removed these paragraphs.

Page 6, line 28 *"For our retrieval ...": please bear in mind that $\gamma_i I$ also works as a regularization term. So, when using Levenberg-Marquardt approach it is incorrect to state that the retrieval is completely unregularized. By the way, it is still not clearly stated if you use the Levenberg-Marquardt term in you approach or not.*

Reply: We do not believe this is correct in the standard use of the term "regularization". The Levenberg-Marquardt term does not appear in the cost function as would a traditional regularization term, and in theory, the retrieval should converge to the same solution (neglecting issues of multiple local minima) with or without the Levenberg-Marquardt term. It is true that the Levenberg-Marquardt term can have a regularization effect if the retrieval is

stopped before proper convergence, but that is not the case here.

Page 7, Eq. (3) *Provide α value.*

Reply: Added.

Page 7, Eq. (3) *The statement " $\mathbf{0}$ indicates a number of zeros equal to the number of altitude grid points" is wrong. It must be the number of altitude grid points minus one.*

Reply: Thank you, this has been corrected.

Page 7, line 4 *There are certainly some good reasons to use zero a priori state vector especially when employing smoothing constraints but the "simplicity" is not really the best one. It should be also mentioned that usage of zero a priori state vector often results in a low bias of the solution.*

Reply: We have removed the word "simplicity". We agree that with certain forms of regularization a zero a priori results in a low bias, however we have not seen anything to suggest that a second derivative constraint results in a consistent low bias. If there is a study that shows this we would be happy to state this and add a reference.

Page 7, lines 9-10 *I do not agree that the resolutions of the vertical and horizontal grids are strictly coupled. In principle any grid combinations can be used, this might require however a stronger regularization as the total amount of information remains the same. The main challenge here is to identify the optimal set of grids and regularization parameters. This set might however depend on the targeted usage of the retrieval data.*

Reply: I think we are mostly in agreement here, when we say the resolutions are coupled we meant to refer to the resolution of the retrieval, not the actual grid. We have changed this to state "the retrieval vertical and horizontal resolutions are inherently coupled together". The main idea we meant to convey is that crudely if we reduce the retrieval vertical resolution, there is more information available for the horizontal part.

Page 7, lines 12-13 *"The effect of a one dimensional retrieval on horizontal regularization...."*

- I guess you mean "horizontal resolution".

Reply: Thank you, this has been changed.

Table 1 *Please provide the reference tangent height for each interval.*

Reply: We have added the normalization altitude for each triplet to the table.

Sect. 2.7.1 *What is the minimum retrieval altitude for ozone?*

Reply: This information is now available much earlier in the revised manuscript.

Page 8, line 7 *Here and further below in the text you are talking about the "atmospheric upwelling". I suppose you mean the upwelling radiation. However, this notation is commonly used in the scientific community to describe the dynamic processes and means the upward moving air masses rather than radiance. Please use another notation throughout the text to avoid a confusion.*

Reply: We have changed all occurrences of "atmospheric upwelling" to "upwelling radiation".

Page 8, lines 20-21 *I guess Eq. (4) is valid for both triplets and doublets. "... for triplet k " in line 21 should be "... for triplet l ".*

Reply: Corrected.

Page 9 *"...any errors in the absolute calibration ..." - this is not completely true for an imaging instrument because the information for different tangent heights comes from different areas of the CCD and can have different calibration errors.*

Reply: This is true but we do not think our statement "helps to minimize any errors in the absolute calibration" contradicts this. The full line in the revised manuscript now reads "The high altitude normalization helps to minimize errors in the absolute calibration of the instrument and reduces the sensitivity to upwelling radiation."

Page 10, Eq, (6) *It is not clear how the second term is employed in the retrieval as the modeled Rayleigh background needs to be subtracted in the same way from both measured*

and modeled radiances and thus is canceled out when calculating $\mathbf{y} - F(\mathbf{x})$ *in accordance with Eq. (2).*

Reply: Thank you, this was confusing in the text. The Rayleigh subtraction is not used in the actual retrieval, although as you pointing out it would have no effect, it is only used to determine the high altitude normalization location based on the procedure of Bourassa et. al. 2012. We have modified the text to make this clear.

Sect. 2.7.2 *No information is provided about how the aerosol extinction coefficient is calculated for other wavelengths.*

Reply: This is done using the same Mie code and assumed particle size distribution as for the phase function, the revised manuscript notes this and adds a reference to the source of the index of refraction data.

Page 11, line 1 *"... albedo is handled in a two-dimensional sense ..." - what is the second dimension for the albedo?*

Reply: We have reworded the first part of this sentence to "While albedo in the forward model is allowed to vary in the horizontal direction".

Sect. 2.7.3 *40 km tangent height to retrieve the surface albedo is quite high. Have you checked a possible influence of the stray light at this tangent height?*

Reply: We have done some internal tests here and have not noticed any significant effect on the retrieved ozone by changing the albedo retrieval height. Many past studies such as Loughman et al. 2005 have found that the absolute value of the retrieved albedo does not have a large effect on the ozone retrieval. Jaross et al. 2014 estimates the stray light contribution to be only 5% at 65 km for 750 nm, so we do not expect a large problem with using 40 km.

Sect. 2.7.3 *The influence of the albedo spectral dependence must be discussed. For example, for a green vegetation the albedo obtained at 745 nm can be very different from that at 602 nm (red edge).*

Reply: We have added a reference to Loughman et. al. 2005 which discusses possible errors associated with neglecting the spectral albedo dependence. However it is important to remember that the albedo is not really surface reflection and is merely an approximation for the unknown diffuse upwelling radiation, thus you would not expect as harsh of a spectral

dependence that you would see with vegetation.

Sect. 3 *The section is unnecessary as all discussed corrections are already implemented in the Level 1 v2.5 dataset of NASA.*

Reply: See our reply to the general comment above.

Sect. 4 *If Levenberg-Marquardt term is used in the retrieval it must be also included in the error analysis.*

Reply: The Levenberg-Marquardt term does not appear in the cost function, and the error analysis is a linearization applied to the cost function so we do not see why this term should appear.

Sect. 4 *Is the signal to noise of 100 is used only in the error analysis or in the standard retrieval as well? Why was not the signal to noise data provided in Level 1 data set used? The latter would provide a realistic instead of maximum error estimation.*

Reply: The SNR of 100 is used in both. The OMPS L1G documentation states that the SNR provided is an "Estimate of detector noise and not an estimate of random measurement uncertainty.", and we were told by the NASA OMPS-LP team that a value of 100 is more realistic.

Page 13, line 9 *Only in the error analysis section the reader learn that the logarithm of the number density is the retrieval parameter rather than the number density itself. This must have been mentioned already in Sect. 2.2.*

Reply: The revised manuscript should correct this.

Page 13, line 14 *what does "but near where the tropopause lowers at midlatitudes" refer to?*

Reply: Reworded to "near where the lower bound of the retrieval changes (due to the lowering tropopause) at mid-latitudes."

Fig. 7 *Suboptimal color scale. How is the sign of the distance from the retrieval location defined?*

Reply: Color scale has been changed. The sign is negative towards the start the start of

the orbit in the southern hemisphere, we have added this to the figure caption.

Page 14, line 3 *"Since the regularization term..." - once again, do not exclude the Levenberg-Marquardt term from the discussion.*

Reply: The Levenberg-Marquardt term does not have any effect here.

Fig. 7 *The definition of the vertically/horizontally integrated averaging kernels is not quite clear. You have a set of averaging kernels for each vertical/horizontal grid point and each of them spans in both vertical and horizontal directions. Is the integration done over these directions? Is yes you seem to show one averaging kernel at each altitude in each panel in Fig. 7? If it was true I would expect the plural in the beginning of line 8 as you show multiple averaging kernels for different altitudes in each panel of Fig. 7. If my understanding of the definition is correct, I would like you to explain why there is a clear maximum at 40 km in tropics and 45 km at mid-latitudes and how it can be interpreted in terms of the retrieval sensitivity.*

Reply: As for the plural vs not plural, Technically there is only one averaging kernel for the entire orbit and what is being shown are multiple rows. We have modified the text to make this clear.

The difference in peak altitude is a little curious, we have two possible explanations. The first reason is that lines of sight below the tropopause are not used in the retrieval. At mid-latitudes we have lines of sight going from 10–18 km, which for the strongest absorbing UV triplets have peak sensitivity in the 40–50 km region owing to the optically thick line of sight path. Since these lines of sight are missing in the tropics the sensitivity peak is lower. Another way of thinking about this is that generally the information content is poorest at the retrieval boundaries, and increases away from them. Since the lower boundary is higher in altitude in the tropics it makes sense that the information maximum shifts downward.

The second cause is the difference in solar zenith angle between the two points. For the OMPS-LP geometry, the tropics have low solar zenith angles with minimal solar attenuation compared to the limb path. Higher latitudes have higher solar zenith angles where solar attenuation becomes more important. It is expected that sensitivity overall shifts upwards in areas with significant solar attenuation as the attenuation happens above the tangent point.

Page 14, line 9 *"Only minor differences ..." - to my opinion the majority of differ- ences occur around 40 km and they are not minor.*

Reply: We see the referees point, however at 40 km the difference in FWHM is less than

25 km. We have reworded the text to state "Only minor differences in the FWHM ..."

Page 14, lines 11-12 *"it was found that ..." - it is hard to believe as it is widely known that the averaging kernels for "relative" retrievals (i.e. retrieval of relative deviations from a priori or logarithms) depend on the atmospheric state. Please provide the averaging kernel plot for different season to justify you statement.*

Reply: We have added a second orbit (from a different season) averaging kernel to the figure. We have also reworded the offending sentence to "it was found that deviations from orbit to orbit are small enough that the above resolution estimates are representative for the entire dataset."

Fig. 7 *why does the tropics plot have a white area below 18 km, how is the lower boundary of the retrieval defined?*

Reply: The data is masked below the lowest retrieval point which is the first altitude above the tropopause, we hope this is clear in the revised manuscript.

Page 14, last paragraph *It is absolutely inappropriate to neglect the instrument field of view without any investigations as it might lead to a significant change in both the retrieval results and error analysis.*

Reply: See the reply to the general comment.

Sect. 5.1 *The results must be provided over the whole orbit as it is essential to estimate how the retrievals compare outside the vortex edge region. Another simulation for a different season with a vortex edge in the northern hemisphere needs to be provided to assess the influence of the viewing geometry.*

Reply: We have modified the first figure to show the entire orbit. We have also added a second simulation for a different season with a strong ozone gradient in the northern hemisphere.

Page 15, line 25 *"For limb scatter measurements ..." - please illustrate this by plotting the averaging kernel for about 65° S and 15.5 km in both horizontal and vertical directions using a proper color scale.*

Reply: While the averaging kernel does also somewhat show this effect (in fact, it only does because some regularization is present) we do not think the requested figure is appropriate

to justify the statement "For limb scatter measurements ozone sensitivity is larger on the instrument side of the line of sight". The averaging kernel is specific to our 2D retrieval, and we are talking about an effect that is retrieval independent. The proper figure is one of the two-dimensional Jacobian for a single line of sight, of which there are many in paper referenced in the text (Zawada et. al. 2017).

Sect. 5.2 *this section is not really informative and can be skipped. Details on the execution time suit better in the algorithm description section.*

Reply: We have removed this section and moved the information into the algorithm description section.

Sect. 5.3 *Not only the anomalies but also the monthly mean values themselves need to be compared. This needs to be done for different latitude bands (tropics, mid-latitudes, high latitudes).*

Reply: See the reply to the general comment above.

Fig. 10 *Why the altitudes above 59 km are not shown? If I understand it correctly, the retrieval runs up to 59 km.*

Reply: We assume the referee means why are altitudes above 50 km not shown. 50 km tends to be a common cutoff for ozone anomaly figures (and trend figures) due to the strong diurnal effect. In the coincident comparisons we can go above 50 km as the time difference between the two measurements is quite small. There are also issues where filtering MLS data according to the recommended procedure frequently cuts the data off $\sim$55 km or occasionally lower, so below 50 km the sampling is roughly consistent for both instruments.

Page 19, lines 1-3 *"... with the horizontal along-track resolution being poorer.." - please provide the values of the resolution and sampling for both instruments.*

Reply: We have added this information to the text.

Page 19, lines 5-6 *".. has been degraded to the MLS pressure grid with a least square fit..." - please clarify what exactly was fitted and how you can degrade the vertical resolution using a least square fit. Here, a convolution with averaging kernels would be more suitable.*

Reply: This is simply the recommended procedure in the MLS data quality document, we have added a reference to the data quality document to indicate this. The OMPS-LP

measurements are converted to pressure at native resolution in pressure, then rather than interpolating these values to the MLS pressure grid a least squares fit is done assuming linear VMR variations. We have opted not to apply the MLS averaging kernels (in addition to the least squares fit) since our vertical resolution (estimated 1–2 km) is not significantly better than the MLS vertical resolution (∼3 km). Futhermore, the MLS averaging kernels are fairly strongly peaked (peak values of 0.6 in the UTLS) so it would not be expected to make any significant differences. Jiang et al. 2007 did compare both of these methods (least squares fit vs averaging kernel) and found negligible differences even when comparing high resolution sonde measurements to a version of the MLS data with poorer vertical resolution than what we are using here.

Jiang, Y. B., et al. (2007), Validation of Aura Microwave Limb Sounder Ozone by ozonesonde and lidar measurements, J. Geophys. Res., 112, D24S34, doi:10.1029/2007JD008776.

Fig. 12 *Provide the lower and upper altitude of the plotted range. Provide the same plot from 1D retrieval. Explain the lower limit of the retrieval.*

Reply: Tick labels have been added for the maximum and minimum of the plotted altitudes. The lower limit is now explained earlier in the revised manuscript. We do not see any value in adding results from the 1D retrieval here. Our only claim made about the 1D retrieval is that it has problems in the presence of large horizontal gradients, of which there are none in this orbit.

It would be also interesting to show some examples from NASA Level 2 data, especially in Fig. 14.

Reply: We agree this would be an interesting study, and in fact we believe there is work being done by other groups on comparing OMPS-LP retrievals by different processors, but we feel it is beyond the scope of this manuscript to include these comparisons.

Technical corrections

Page 2, Eq. (1) *matrices have to be shown in bold face to match the corresponding notations in the text.*

Reply: Corrected, thank you.

Page 15, line 5 *duplicated word "those".*

Reply: Corrected, thank you.

We would like to thank the referee for their helpful comments and suggestions. Included below is each of the referee's comments (italics) followed by our reply.

Responses to Anonymous Referee 2

General Comments

---

in the first algorithm description sections authors provide rather theoretical description of the inversion method without stating what physical quantities are used as measurement and what exactly are going to be retrieved. Only very late and in differenent places it is said that state vector may consist of various quantities in a sequence, e.g. logarithm of number density (stated only on page 13 of the manuscript), perhaps aerosol number density (but it is not clearly stated in Sect. 2.7.2). This makes it hardly possible to follow the arguments about practical considerations provided along the theoretical descriptions. I would strongly encourage the authors to restructure the manuscript to make its understanding straight forward.

Reply: Thank you for the suggestion, we agree in many places there was too much general information. In the revised manuscript specifics about the state vector (such as that it is logarithm of number density) appear much earlier. Some of the general information has been removed and/or replaced with specifics about the retrieval for OMPS-LP. We have also rearranged some sections so that information about the specific species retrievals (ozone, aerosol, albedo) appears earlier.

I have a feeling that more should be done with respect to the verification/validation, especially under strong gradient conditions. There is only one such orbit provided. Please add a study for a northern winter day with strong northern polar ozone deple- tion. For this case the Suns geometry is opposite to that of the gradient in the SH. Also gradient at high SZAs (see below) must be investigate to sustain statements in the manuscript. Additionally middle and high latitudes where much stronger ozone variations might take place as at equator must be covered in a more systematic way. One could at least provide comparisons for one orbit per season thus covering typical seasonal variations in ozone distribution.

Reply: We have added a second simulated orbit where there is strong ozone depletion in the northern hemisphere. We agree that there is a lot of potential validation work left to do for the dataset but we believe it is beyond the scope of the manuscript. As stated in the text, we are planning on doing doing an in-depth validation in a future study, what is presented here is preliminary efforts in this direction. We have replied to the referees comment concerning gradients at high solar zenith angles in the specific comments below.

---

there is a constant signal to noise ratio 100 assumed for the whole scan profile for the

error estimation as given in conclusions of Jaross et al., 2014. Some sceptics is there due the natural illumination changes of several magnitudes along the tangent altitude and even despite the applied dynamical considerations, stray light and possible degradation of the instrument might be an issue.

Reply: This could certainly be the case, but currently the estimate given in Jaross et al., 2014 remains the best available estimate for the instrument performance. The effect of illumination changing by several orders of magnitude is somewhat mitigated by the OMPS-LP instrument which collects two interleaved images of the full scene with different integration times and aperture sizes. It does appear that the final error analysis results are however at least somewhat reasonable from the standard deviation of the MLS comparisons.

Specific Comments

P1L6 *Add some words that MLS measurements used for the comparison are as well 2D, tomographic.*

Reply: Added

P1L24 *add "and OClO" after "of NO2" since Pukite et al., 2008 did 2D retrieval for this gas as well.*

Reply: Added

P2L3 *"relatively fast along orbital track sampling": fast relates to speed or time, perhaps say "relatively fine resolved".*

Reply: Changed

Sect.2. *As said in general comments; it would help a lot to state at the beginning what physical quantities you are operating with.*

Reply: This is done in the revised manuscript.

P3L7 *"Between grid points bi-linear interpolation is applied to create a continuous representation of the atmosphere." It must be explained in detail how the interpolation is implemented. I.e. this could mean some subgridding or analytic constrains in model.*

Reply: This is a good point. We have moved this statement to the forward model section

to make it clear this is something internal to the forward model. The exact procedure in which this is done is described in detail in Zawada et al. 2015.

P3L15, F1 *Figure must be improved. Please use different colors as "white grey" and other grey since it is really impossible to distinguish in the figure.*

Reply: We have changed the two colors to red and gray.

P3L17 *"A common approach to minimize" Citations needed*

Reply: We have added a reference to Rodgers (2000).

P4L1-2 *"Under this approach we have not noticed unphysical effects at the edges of the retrieval." A prove for this statement is necessary. Given your verification and validation evidence (just one orbit with gradient at lower SZA) this has not been verified: Can this been tested with an example with a gradient condition at the orbit parts with SZA 88 deg and above? In such cases Pukite et al. 2008 reported problems for the first profile of the orbit. Please provide evidence.*

Reply: In the shown orbit there are natural gradients in the ozone field at gradients above 88 SZA, we have not artificially suppressed them. We have extended this orbit to the full range (rather than just the southern hemisphere) as well to see both edges of the retrieval. We have also added a second simulated orbit with gradient conditions in the northern hemisphere, and in none of these cases have we noticed significant edge effects. However it is true that if there was a large, ozone hole in magnitude, gradient occurring at 88 SZA (typically does not happen with the OMPS-LP geometry) we would expect some edge effects to occur. We have changed the offending statement to read "Under this approach for typical conditions we have not noticed unphysical effects at the edges of the retrieval, but this is still under investigation."

P4L10 *Related to general comments. Still on the 4th page of the manuscript there is no idea what is to be state vector and measurement vector.*

Reply: This should be better in the revised manuscript, see reply to the general comment.

P4L18 *A more concrete and exact description is needed. How the transformation is practically performed? What assumptions used? What has to be understood under "atmosphere specified on the retrieval grid is transformed", i.e. What is this atmosphere consisting from and characterized by? What and how it is changed due to transformation? How the Jacobian*

matrix is transformed?

Reply: This section was poorly worded and has mostly been removed at the request of the other referee. All that is done is a linear change of coordinates from the plane containing the lines of sight to the orbital track (retrieval grid). We have moved the information about the mismatch between the line of sight plane and the retrieval grid to the state vector section.

P4L21 *"These transformations are typically quite small in effect" Can you provide a number?*

Reply: We have added the statement that at the equator the mismatch between the line of sight plane and the orbital plane is approximately 5°.

P5L6 *And how much time resource do you need for one orbit?*

Reply: This information was stated later in the manuscript. In the revised manuscript we have moved the example retrieved orbit section (which stated the approximate time per orbit) into the algorithm section.

P6L16 *"Most atmospheric retrieval methods fall into two classes" Again, it is of course good to give some review about the background of inverse methods but it is difficult for a reader to follow your considerations and choices if it is still not stated what you are going to retrieve from what.*

Reply: This section has been removed at the request of the other referee.

P6L17 *"the resolution of the retrieved profile is determined by ... the resolution of the retrieval grid." This statement is generally wrong: The resolution is an ability to resolve some features. If there is not enough information one is not able to resolve the features even on fine grid. I think you wanted to say something else; perhaps one should skip the part of the sentence after "i.e."*

Reply: At the request of the other referee we have removed this section so this is not an issue anymore. However, if we define resolution from the averaging kernel then as long as $K^T S_\epsilon^{-1} K$ is invertible then this is a true statement. So the referee is correct in that the grid can not be made arbitrarily fine, but if $K^T S_\epsilon^{-1} K$ is singular then the retrieval cannot be done without regularization anyways.

Eq.3 *shouldnt all zeros be bold?*

Reply: We think it is correct the way it is. The non-bold zeros are needed to separate

different altitudes.

P7L16 *"ozone number density, stratospheric aerosol number density, and surface reflectance assuming a Lambertian surface" Later you state that the state vector for ozone retrieval is logarithm of number density. This is again the confusion here between the long theory description and rather imprecise and misplaced description of the practical stuff.*

Reply: This should be improved in the revised manuscript, these statements have been moved earlier with much of the general information changed to OMPS-LP specific information.

P7L19 *Does it mean solving 3 different separate inverse problems (Eq. 2)?*

Reply: Yes for three separate inverse problems, but the albedo retrieval does not use Eq. 2.

P8L20-21, Eq4 *In text you mention k to be used for both indexing tangent altitude and triplet, though in Eq. (4) indexing for triplets is missing.*

Reply: Thank you, this has been corrected.

P8L22 *What is meant by ozone sensitivity is minimal? Or perhaps effect of ozone absorption on spectra is minimal?*

Reply: We have reworded this to "where the effect of ozone absorption on the observed radiance is minimal."

P13L8 *"signal to noise ratio of 100"; "an upper bound on the error estimate taken from Jaross et al. (2014)." As said at the beginning this assumption might be much too optimistic.*

Reply: See the reply to the general comment

P13L9 *"state vector is the logarithm of number density". Only on page 13 there is finally mentioned the physical quantity all about the theory was. What about other quantities?*

Reply: Description of the state vector has been improved, this information appears much earlier in the revised manuscript.

P14 *Have you studied the effect different settings of the horizontal regularization. Is it not*

possible to do retrieval without any horizontal regularization because you also match the horizontal retrieval grid to that of the measurements?

Reply: We have been looking into this. It is possible to do the retrieval without regularization, however there end up being unphysical oscillations in the horizontal direction. The exact cause of the oscillations is still being investigated but it would not be unexpected for a retrieval where the sampling matches the retrieval grid to have oscillations in that dimension. We chose the current level of regularization somewhat conservatively to remove the oscillations, and we plan to further study this for a future version of the retrieval.

P15L28 *"orbit 27695" mention here day and time of the Eq. crossing.*

Reply: Added

P17L7 *"Figure 10 shows the result of these comparisons in the tropical* 5° *S to* 5° *N latitude bin." What is about systematic study for other latitudes where far more gradients appear?*

Reply: A full systematic validation of the dataset is intended for a future validation paper.

P19L10 *day, time for orbit?*

Reply: Added

P23L4 *"for the entire orbit" The retrieval is limited to SZA 88 deg. This should be stated.*

Reply: Thank you, we have added this.

P23L13 *"one orbit" You compared two orbits.*

Reply: Thank you, changed.

P23L18 *"tradiational"-¿ "traditional"*

Reply: Thank you, corrected

Tomographic retrievals of ozone with the OMPS Limb Profiler: algorithm description and preliminary results

Daniel J. Zawada[1], Landon A. Rieger[1], Adam E. Bourassa[1], and Douglas A. Degenstein[1]

[1]University of Saskatchewan

Correspondence to: Daniel J. Zawada (daniel.zawada@usask.ca)

Abstract. Measurements of limb scattered sunlight from the Ozone Mapping and Profiler Suite Limb Profiler (OMPS-LP) can be used to obtain vertical profiles of ozone in the stratosphere. In this paper we describe a two-dimensional, or tomographic, retrieval algorithm for OMPS-LP where variations are retrieved simultaneously in altitude and the along orbital track dimension. The algorithm has been applied to measurements from the center slit for the full OMPS-LP mission to create the publicly available USask OMPS-LP 2D v1.0.2 dataset. Tropical ozone anomalies are compared with measurements from the Microwave Limb Sounder (MLS) where differences are less than 5% of the mean ozone value for the majority of the stratosphere. Examples of near coincident measurements with MLS are also shown, and agreement at the 5% level is observed for the majority of the stratosphere. Both simulated retrievals and coincident comparisons with MLS are shown at the edge of the polar vortex, comparing the results to a traditional one-dimensional retrieval. The one-dimensional retrieval is shown to consistently overestimate the amount of ozone in areas of large horizontal gradients relative to both MLS and the two-dimensional retrieval.

1 Introduction

The Ozone Mapping and Profiler Suite Limb Profiler (OMPS-LP) on-board the Suomi-NPP spacecraft began taking routine measurements of limb scattered sunlight in early April 2012 (Flynn et al., 2006). The limb profiler images the atmospheric limb every $19\,\mathrm{s}$ ($\sim$$125\,\mathrm{km}$ along track) from the ground to approximately $100\,\mathrm{km}$ using three vertical slits that are separated horizontally by $4.25°$. A prism disperser is used to obtain a spectrally resolved signal in the range 290–1000 nm. These spectrally resolved measurements can be inverted with a forward model accounting for multiple scattering to obtain vertically resolved profiles of ozone concentration in the atmosphere.

The standard OMPS-LP ozone product is produced by NASA and version 1.0 of the retrieval is described in detail by Rault and Loughman (2013). The NASA retrieval employs the assumption of horizontal homogeneity, treating each vertical image separately to retrieve a one-dimensional vertical profile. However, it is possible to take advantage of the long limb path length and fast sampling capabilities of OMPS-LP to combine multiple images together and retrieve in the orbit track and altitude dimensions simultaneously. These two-dimensional, or tomographic, retrievals have been used successfully in many retrievals from limb emission instruments (e.g. Degenstein et al., 2003, 2004; Livesey et al., 2006; Carlotti et al., 2006). A two-dimensional retrieval of NO_2 and $OCLO$ was done for limb scatter measurements from the SCanning Imaging Absorption SpectroMeter for Atmospheric CHartographY (Bovensmann, 1999) by Pukīte et al. (2008) and a preliminary two-dimensional retrieval study

for ozone using a single scatter radiative transfer model was also performed by Rault and Spurr (2010) using simulated OMPS-LP measurements. Measurements from OMPS-LP are a natural candidate to attempt a two-dimensional retrieval due to the relatively ~~fast along~~ fine resolved orbital track sampling ($\sim$125 km) compared to other limb scatter instruments, for example, the Optical Spectrograph and InfraRed Imaging System (OSIRIS) (Llewellyn et al., 2004) has $\sim$600 km along track sampling.

In this paper we describe a retrieval algorithm for the central slit of OMPS-LP which accounts for inhomogeneity in the along orbit direction, and present preliminary results. To the author's knowledge this is the first two-dimensional limb scatter ozone retrieval applied to real measurements. The algorithm is described in detail in Sec. 2. We have applied the algorithm to the entire mission of OMPS-LP, creating a dataset of vertical profiles of stratospheric ozone from early 2012 to present with near global coverage (USask OMPS-LP 2D v1.0.2 dataset). Section 5 presents some preliminary results and validation efforts with the dataset. The dataset is compared against the also two-dimensional ozone retrievals (Livesey et al., 2006) from the Microwave Limb Sounder (Waters et al., 2006). Tropical ozone anomalies are compared against those from ~~the Microwave Limb Sounder (MLS) (Waters et al., 2006)~~ MLS for the full mission dataset. Lastly, nearly perfect coincident measurements with MLS are investigated.

2 The retrieval algorithm

2.1 Overview

Here we follow the optimal estimation framework outlined in Rodgers (2000) and use similar notation. The general goal of the atmospheric inverse problem is to find the optimal set of state parameters, $\boldsymbol{x}$, given with a set of measurements, $\boldsymbol{y}$, and other apriori information or constraints. The vector $\boldsymbol{x}$ of length n is often called the state vector, while the vector $\boldsymbol{y}$ of length m is called the measurement vector. ~~One approach to this problem~~ In our OMPS-LP ozone retrieval case, $\boldsymbol{x}$ consists of the logarithm of ozone number density on a two-dimensional grid (altitude and along the orbital track), and $\boldsymbol{y}$ contains the logarithm of the spectrum for multiple OMPS-LP images at select ozone sensitive wavelengths. A common approach to the inverse problem (Rodgers, 2000) is to minimize the cost function,

$$\chi^2 = [F(\boldsymbol{x}) - \boldsymbol{y}]^T S\mathbf{S}_\epsilon^{-1}[F(\boldsymbol{x}) - \boldsymbol{y})] + [\boldsymbol{x}_a - \boldsymbol{x}]^T R\mathbf{R}^T R\mathbf{R}[\boldsymbol{x}_a - \boldsymbol{x}], \tag{1}$$

where $\mathbf{S}_\epsilon$ is the covariance of the measurement vector, $\mathbf{F}$ is the forward model, $\mathbf{R}$ is a regularization matrix, and $\boldsymbol{x}_a$ is the apriori state vector. Apriori information is included through the two quantities R and x_a. Applying a standard Guass-Newton minimization approach to the cost function results in the iterative step,

$$\boldsymbol{x}_{i+1} = \boldsymbol{x}_i + (\mathbf{K}_i^T\mathbf{S}_\epsilon^{-1}\mathbf{K}_i + \mathbf{R}^T\mathbf{R} + \gamma_i\mathbf{I})^{-1}\cdot \left[\mathbf{K}_i^T\mathbf{S}_\epsilon^{-1}(\boldsymbol{y} - \mathbf{F}(\boldsymbol{x}_i)) - \mathbf{R}^T\mathbf{R}(\boldsymbol{x}_i - \boldsymbol{x}_a)\right], \tag{2}$$

where $\mathbf{K}$ is the Jacobian matrix of the forward model, i is the iteration number, and γ_i is a Levenberg-Marquardt damping parameter. ~~The~~ A relatively small Levenberg-Marquardt type ~~regularization term $\gamma_i I$ may be~~ term, $\gamma_i = 0.1\cdot$ the mean value of

the diagonal of $\mathbf{K}_i^T \mathbf{S}_\epsilon^{-1} \mathbf{K}_i$, is included to move the solution step closer to that of a gradient descent method, aiding performance when the Gauss-Newton step is outside the linear regime.

Equation (2) forms the basis of the retrieval method used in this work.

The tomographic or two-dimensional nature of the retrieval is encoded in the details of the definitions of the state vector and the measurement vector. The state vector contains information about the atmospheric state for an entire orbit of OMPS-LP and is described in detail in Sec. 2.2. A brief description of the forward model, which must account for atmospheric variations along the line of sight, is given in Sec. 2.3 and Sec. 2.5. The ~~form of regularization and apriori used is given in Sec. 2.9~~exact form of the measurement vector for ozone and minor retrieved species (stratospheric aerosol and surface albedo) are presented in Secs. 2.7 and 2.8 respectively. Lastly, the form of ~~the measurement vector for each retrieved species is presented~~ regularization and apriori used is given in Sec. ~~2.6~~2.9.

For this work v2.0–2.4 of the OMPS-LP L1G product (https://ozoneaq.gsfc.nasa.gov/data/omps/) is used.

2.2 The state vector

The state vector ~~is a representation of the atmospheric state~~ consists of the logarithm of ozone number density on a discrete grid, ~~which we will refer~~ referred to as the retrieval grid. The retrieval grid ~~consists of a set vertical profiles at discrete locations~~ is two-dimensional in altitude and angle along the orbital ~~track of the instrument's tangent point. Between grid points bi-linear interpolation is applied to create a continuous representation of the atmosphere. The state vector for a single trace species is a flattened representation of this grid, with altitude being the leading dimension. As~~ plane of OMPS-LP~~measures scattered sunlight, each orbit has a natural start and stop point characterized by high solar zenith angles.In constructing the retrieval grid we use images with solar zenith angles at the tangent point of less than 88°.~~

~~Figure 1shows an illustration of the constructed retrieval grid~~ , and ~~its relation to measurements from OMPS-LP. The horizontal resolution~~ is shown in Fig. 1. The altitude component of the grid is discretized in 1 km steps with lower and upper bounds at the tropopause altitude and 59 km respectively.

The horizontal spacing of the retrieval grid is chosen to match the horizontal sampling of OMPS-LP, which is approximately 125 km. A consequence of the ~~limb~~ OMPS-LP viewing geometry is that measurements with a higher tangent point are closer to the instrument than measurements with a lower tangent point. For convenience the absolute locations of the horizontal retrieval grid locations (~~white~~ gray lines in Fig. 1) is chosen to match the average tangent point of each measurement image. As OMPS-LP measures scattered sunlight, each orbit has a natural start and stop point characterized by high solar zenith angles. In constructing the retrieval grid we use images with solar zenith angles at the tangent point of less than 88°.

A consequence of performing a tomographic retrieval is that there is less information at the edges of the retrieval grid, simply because there are less measurements which sample near the edges. ~~A common approach to minimize this effect is to cut off the ends of the retrieval, e.g. retrieve on a grid from 0° to 100° but only report the results for 5° to 95°. This approach works well when the next retrieval starts where the first one ended, here one may allow some overlap between the two retrievals, throwing out both edges and merging the results together. The final result would be nearly eliminating the edge effects for a small cost~~

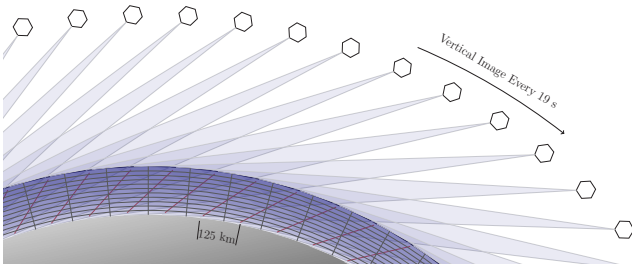

Figure 1. Conceptual image (not to scale) of the OMPS-LP viewing geometry and retrieval grid. The retrieval grid locations (~~white~~ gray lines) are chosen to match the average tangent point of the OMPS-LP measurements (~~solid black~~ red lines).

~~in increased computational time. However, if the edge is a physical limit for the retrieval, as is the case for this retrieval, then cutting off the ends of the retrieval will result in a loss of data.~~

~~In order to maximize the amount of data retrieved in the OMPS-LP retrieval, we use a similar but different approach.~~ As previously mentioned, our retrieval grid has hard cutoffs at solar zenith angle 88°. However, when constructing the measurement vector we use all images with solar zenith angle less than 90°. Under this approach for typical conditions we have not noticed unphysical effects at the edges of the retrieval, but this is still under investigation. However there is still less information present at the retrieval boundaries, which is reflected in the resolution and precision estimates described in Sec. 4. The latitudinal coverage of OMPS-LP, and thus the retrieval grid, varies throughout the course of the year as the illuminated portion of the Earth changes. The latitude region 60° S to 60° N is sampled near continuously throughout the year, while coverage extends to 82° in each hemisphere's summer.

Due to the Earth's rotation, there is a slight mismatch between the line of sight plane and the retrieval grid as is shown in Fig. 2. At the equator the approximate mismatch is 5°, resulting in a ∼10 km horizontal distance between the next image's average tangent point and the previous image's line of sight plane. The effect is largest at the equator with the mismatch almost completely disappearing at the northern and southernmost parts of the orbit (82° N and 82° S). To perform the retrieval, the horizontal component of the line of sight plane for every image is projected onto the horizontal component of the retrieval grid (orbital track dimension).

2.3 The forward model

The forward model used in this study is SASKTRAN-HR (Bourassa et al., 2008; Zawada et al., 2015). SASKTRAN-HR solves the radiative transfer equation in integral form using the method of successive orders initialized with the incoming solar irradiance. The model is capable of handling inhomogeneities in the atmospheric state in the along line of sight direction. Internally the forward model performs bi-linear interpolation between grid points to create a continuous representation of the atmosphere. In addition to radiance, the model also outputs the Jacobian matrix with respect to the underlying two-dimensional atmosphere. Jacobians are calculated analytically taking into account all first order of scatter terms with approximations made

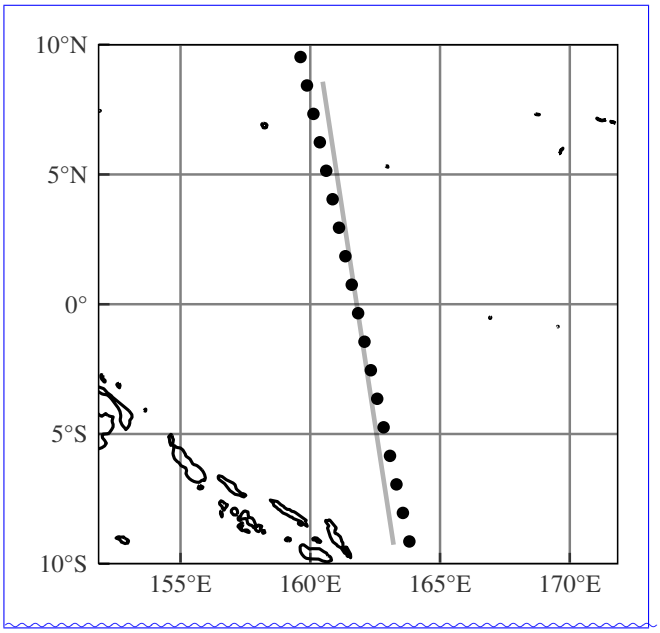

Figure 2. Example of mismatch between the line of sight plane and the tangent point ground track. Black dots show the tangent points (at 25 km) for OMPS-LP orbit 14940. The gray line represents the line of sight plane for the tangent point intersecting the line.

for higher order terms. The forward model and the Jacobian calculation are described in depth in Zawada et al. (2015) and Zawada et al. (2017) respectively.

~~Due to the Earth's rotation, there is a slight mismatch between the line of sight plane and the retrieval grid as is shown in Fig.2. The horizontal distance between the next image's average tangent point and the previous image's line of sight plane is approximately ~10 km near the equator, with the effect diminishing near the poles. Since SASKTRAN-HR specifies the atmosphere in the line of sight plane, some transformations need to be performed during the retrieval process. At the beginning of each iteration, the atmosphere specified on the retrieval grid is transformed to the internal SASKTRAN-HR representation. The radiative transfer calculation is then performed, obtaining both the radiance and the Jacobian matrix. Since the Jacobian matrix was calculated on the internal SASKTRAN-HR atmosphere grid, this needs to be transformed back to the retrieval grid representation. These transformations are typically quite small in effect, and are done taking into account the symmetries that SASKTRAN-HR assumes in the radiative transfer calculation.~~

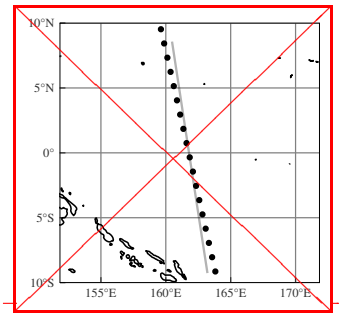

~~Example of mismatch between the line of sight plane and the tangent point ground track. Black dots show the tangent points (at 25 km) for OMPS-LP orbit 14940. The gray line represents the line of sight plane for the tangent point intersecting the line.~~

2.4 Computational considerations

In a tomographic retrieval, the length of the state vector, n, and the length of the measurement vector, m, are significantly larger than those of a one-dimensional retrieval. For example, if the retrieval grid was set up to match the inherent resolution of the OMPS-LP measurements of a single orbit, for each species n would be on the order of 10000, and for each wavelength m would also be on the order of 10000. Storing these vectors does not pose any computational challenge, however, it quickly becomes necessary to store the $m \times n$ Jacobian matrix using sparse storage techniques. The Jacobian matrix is naturally sparse in the horizontal direction as sensitivity is largest at the tangent point and decreasing away from it. For the limb scattering problem involving multiple scattering elements of the Jacobian matrix are never truly zero, every point in the atmosphere should in theory contribute to every measurement. However, owing to the approximations made in the Jacobian calculation outlined in the section prior, contributions are only calculated along the line of sight and solar planes resulting in a sparsity factor of $\sim$0.05. The sparsity of the Jacobian matrix can be improved by artificially allowing only profiles less than some specified distance to the tangent point to contribute, as is done in Livesey et al. (2006). For our retrieval we limit each measurement to contribute to profiles within 10° of the tangent point.

While every matrix in Eq.(2) is sparse, it is often desirable from a computational speed point of view to store some combinations of matrices densely. In particular, solving the linear system requires computing the $n \times n$ $(\mathbf{K}_i^T \mathbf{S}_\epsilon^{-1} \mathbf{K}_i + \mathbf{R}^T \mathbf{R} + \gamma_i \mathbf{I})$ matrix. While still somewhat sparse, we have observed significant speed increases by solving the linear system densely. For a full OMPS-LP orbit this matrix would be 10000×10000, taking less than 1 GB of memory.

2.5 Accounting for the time dependence

Due to an inadequate amount of measurements we do not account for the time variation of the ozone field in the retrieval. The reported time for each retrieved profile is calculated by interpolating the measurement times on the tangent points to the retrieval grid. While not perfect, we expect this is a good estimate as the majority of information for a single retrieved profile originates from the images that have tangent points near it. Nevertheless, there are several other time dependent effects which play a role in how the retrieval is performed.

The radiative transfer equation is explicitly time dependent owing to the changing solar conditions. For an imaging instrument such as OMPS-LP, the natural and most accurate solution to this problem is to re-run the forward model for every image. That being said, there is potential for large computational speed improvements by combining multiple images into the same forward model calculation. Since SASKTRAN-HR solves the radiative transfer equation in a region of interest (nominally a 10° cone with the vertex at the Earth's center, but this can be configured) around the tangent point, there is considerable overlap between the field of interest of one image to the next. However, there are issues in performing this combination:

1. Each image happens at a different instant in time, thus the solar conditions have changed.
2. SASKTRAN-HR's internal atmosphere is specified as a plane in the along line of sight direction. The lines of sight from one image do not necessarily lie in the same plane as the lines of sight for the next image. Furthermore, the more images that are combined together the larger this plane will diverge from the retrieval grid.
3. The Earth is represented internally as a sphere with curvature matching a reference ellipsoid at the average tangent point which changes from image to image.

The first and the third conditions are not unique to tomographic retrievals, limb scanning instruments face similar challenges in one-dimensional retrievals. For example, a single OSIRIS limb scan sequence takes approximately 90 s and is modeled with a single forward model calculation in operational retrieval algorithms (Degenstein et al., 2009). Internal tests have been performed to quantify the three conditions by comparing results that modeled every image separately with retrievals that combined 5 subsequent images together (95 s variation from the first image to the last image) which resulted in mostly random differences in retrieved ozone on the order of 0.5%.

2.6 ~~Regularization~~

~~Most atmospheric retrieval methods fall into two classes, the first is where no regularization term (R in Eq. (2)) is used. In this case the resolution of the retrieved profile is determined by how the state vector is defined, i.e., the resolution of the retrieval grid. It is always desired to make the retrieval grid as fine as possible, but one has to be careful as to not make the grid too fine, allowing over-fitting. In the one-dimensional case retrievals that operate without regularization commonly choose the vertical grid to match the sampling resolution of the instrument. A large advantage of this approach is that the retrieval resolution stays constant over time, side-stepping problems when looking for small changes in a long time series.~~

~~The second approach is to make the retrieval grid finer than the expected resolution of the retrieval, and include some form of regularization in Eq. (2). Regularization acts to include some additional information in the retrieval. If the added information is correct, then the retrieval results in the optimal solution, however this is rarely the case. The additional information could be in the form of an a priori atmospheric state with associated covariance, or it could take the form of an ad-hoc constraint. Common constraints are to impose a cost on the first or second derivative of the state vector. While these constraints do not have a formal justification, they do have some physical basis in that it is expected the retrieved profile be continuous.~~

~~For our retrieval we use a combination of both of the above methods. Since the vertical direction is typically what limb geometry measurements are designed to target, we apply a second derivative constraint only in the horizontal direction of the~~

retrieval grid. The regularization matrix takes the form,

$$R = \alpha \begin{pmatrix} -\frac{1}{4} & \mathbf{0} & \frac{1}{2} & \mathbf{0} & -\frac{1}{4} & 0 & 0 & \dots \\ 0 & -\frac{1}{4} & \mathbf{0} & \frac{1}{2} & \mathbf{0} & -\frac{1}{4} & 0 & \dots \\ 0 & 0 & -\frac{1}{4} & \mathbf{0} & \frac{1}{2} & \mathbf{0} & -\frac{1}{4} & \dots \\ \vdots & \vdots & \vdots & \vdots & \vdots & \vdots & \vdots & \ddots \end{pmatrix},$$

where α is a constant scaling factor used to control the amount of regularization and $\mathbf{0}$ indicates a number of zeros equal to the number of altitude grid points. For simplicity the apriori state vector of Eq. (2) is chosen to be 0. As the regularization matrix used only applies in the horizontal direction, the horizontally integrated vertical resolution of the retrieved profiles matches the vertical resolution of the retrieval grid.

It should be noted that even though we apply no constraints in the vertical direction, the retrieval software is capable of doing so. While the above discussion treats the horizontal and vertical dimensions of the grid as separate entities, their resolutions are inherently coupled together. A lower resolution horizontal grid allows for a higher resolution vertical grid, keeping the total information content relatively constant, and vice-versa. We make no claims on what is the optimal relationship between these two resolutions, and it is something that we are actively investigating. It is important to mention that a one-dimensional retrieval makes the trade-off decision for you, allowing control of only the vertical constraint. The effects of a one-dimensional retrieval on horizontal regularization has been studied for the Michelson Interferometer for Passive Atmospheric Sounding by von Clarmann et al. (2008).

2.6 Retrieval ordering

The retrieval is performed for three major parameters: ozone number density, stratospheric aerosol number density, and surface reflectance assuming a Lambertian surface. While considerable effort has been put into both the aerosol and surface reflectance retrievals, they are performed primarily as a second order correction for the ozone retrieval. Each species is retrieved independently, i.e., holding the other parameters fixed; but the overall retrieval operates in stages, feeding the results of previous parameter retrievals into the current one. The general retrieval order follows that of Degenstein et al. (2009) and is first surface reflectance, then aerosol number density, and then lastly ozone number density. Two passes of this overall procedure are performed, allowing results from the ozone retrieval to couple back into the other retrievals. The first pass of the procedure can be thought of as obtaining a good first guess for state vectors, while the second pass finalizes the retrieval.

A fixed number of iterations is performed in each of the passes. The first round of the retrieval procedure performs five iterations for each of the targeted quantities while the second round performs two iterations. Various diagnostic information is also calculated, including the normalized χ^2 value and the expected χ^2 value at the next step assuming the problem is linear. At the end of the fixed number of iterations it was found that these two values always match within 1%, indicating that the solution has likely converged. It is planned for a future version of the retrieval software to stop early if convergence is detected, however this is not expected to improve the solution only the computational efficiency.

Ozone Sensitive Wavelength [nm]	Reference Wavelength(s) [nm]	Valid Altitudes [km]	Normalization Altitude [km]
292.43	350.31	22–59	60
302.17	350.31	22–55	56
306.06	350.31	22–51	52
310.70	350.31	22–48	49
315.82	350.31	22–46	47
322.0	350.31	22–42	43
331.09	350.31	22–39	40
602.39	543.84, 678.85	0–30	31

Table 1. Wavelength triplet/doublets used in the ozone retrieval.

2.6.1 ~~Ozone~~

2.7 Ozone Measurement Vector

The ozone retrieval uses a common technique first suggested by Flittner et al. (2000) where ozone sensitive wavelengths in the Hartley-Huggins and Chappuis bands are normalized by both ozone insensitive wavelengths and high altitude measurements. This technique, sometimes referred to as the triplet or doublet method, has been used successfully in a variety of limb scatter ozone retrievals (e.g. von Savigny et al., 2003; Loughman et al., 2005; Rault, 2005; Degenstein et al., 2009; Rault and Loughman, 2013). The ozone cross section used in the retrieval is compiled from Daumont et al. (1992); Brion et al. (1993); Malicet et al. (1995). While the triplet/doublet method has previously only been implemented for one-dimensional retrievals, many of the ideas are still applicable to two-dimensional retrievals with some modifications.

Our ozone measurement vector consist of 7 doublets in the Hartley-Huggins absorption bands and one triplet in the Chappuis absorption band shown in Table 1. In one-dimensional retrievals the UV doublets are often forced to only contribute when the atmosphere is optically thin, i.e. when the area of maximal sensitivity is at the tangent point. This can be done through either analyzing the diagonal elements of the Jacobian matrix directly (Loughman et al., 2005), or by only using altitudes above the "knee" of the atmosphere as is done in Degenstein et al. (2009). The primary reason to do this forcing is so that the retrieval is most sensitive to the tangent point, to minimize the effect of the implicit horizontal homogeneity assumption. Since the assumption of horizontal homogeneity is broken for the tomographic retrieval, we allow all UV doublets to contribute down to some minimum altitude, chosen to be 22 km. This altitude is approximately the knee of the 350 nm radiance profile, as seen in Fig. 3, radiances below this altitude are heavily sensitive to ~~atmospheric upwelling~~ upwelling radiation and in particular absorbing aerosols.

The unnormalized measurement vector, $\tilde{y}$, is given by,

$$\tilde{y}_{jkl} = \frac{1}{n_{\mathrm{ref}_l}} \sum_{\lambda \in \mathrm{ref}_l} \log\left[I_j(h_k,\lambda)\right] - \frac{1}{n_{\mathrm{sens}_l}} \sum_{\lambda \in \mathrm{sens}_l} \log\left[I_j(h_k,\lambda)\right], \tag{3}$$

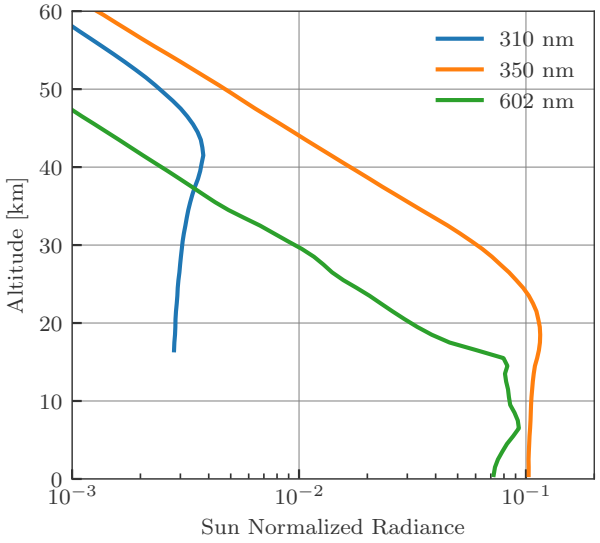

Figure 3. Sun normalized radiances observed by OMPS-LP event number 90 of orbit 19490.

where j indexes image along an orbit, k indexes tangent altitude, l indexes the triplet, and the sets ref_l and sens_l are the reference and sensitive wavelengths for triplet ~~k~~ l from Table. 1 with corresponding lengths n_{ref_k} and n_{sens_k} respectively. Each triplet/doublet is normalized by its value at a high altitude where the ~~ozone sensitivity~~ effect of ozone absorption on the observed radiance is minimal. The high altitude normalization helps to minimize ~~any~~ errors in the absolute calibration of the instrument and reduces the sensitivity to upwelling radiation. The normalization altitude varies for each doublet/triplet (shown in Table 1), and is pushed low to minimize stray light errors.

To avoid discontinuities caused by suddenly introducing UV triplets near 22 km, the diagonal of the measurement error covariance matrix is artificially scaled during the retrieval,

$$S_{\epsilon,ii} = \frac{S_{\epsilon,ii}}{w^2}, \tag{4}$$

where the weights, w, are only applied to the UV triplets and only depend on altitude. The applied scale factors are shown in Fig. 4.

The initial guess for the ozone profile is taken from McPeters et al. (1997), we have observed negligible dependence on the choice of initial state (typically less than 1% on the retrieved ozone values).

Figure 5 shows the retrieved ozone number density for OMPS-LP orbit 27695 (March 2nd, 2017, 10:30 AM UTC at equator crossing). Several low ozone filaments above the ozone layer are visible in both the southern hemisphere and northern hemisphere tropics/mid-latitudes. In the northern hemisphere a low pocket of ozone can be seen below and intruding into the ozone layer.

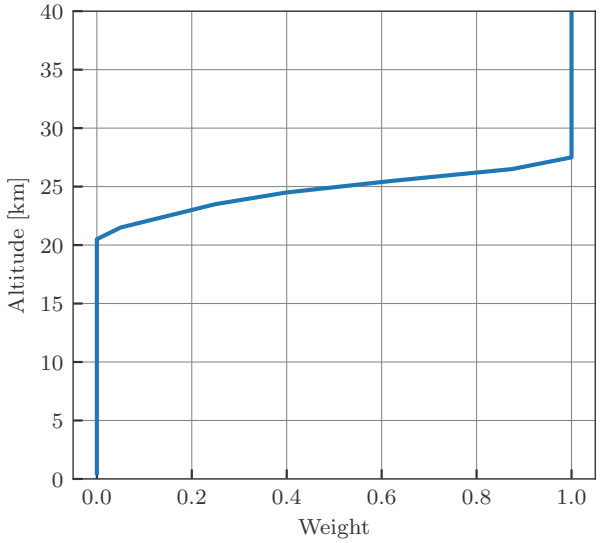

Figure 4. Scaling factors as a function of altitude applied to the UV doublet measurement error covariances.

Processing of this orbit took approximately 124 minutes using 8 threads on an i7-4770k cpu. There were 159 vertical images of radiance data input to the retrieval, giving an approximate processing time of 47 seconds per vertical image. Thus performing the 2D retrieval is not onerous from a computational point of view, two machines of similar computational power are sufficient to keep up to date with routine processing.

2.8 Minor Retrieved Species

2.8.1 Stratospheric aerosol

The stratospheric aerosol measurement vector definition follows closely the one outlined in Bourassa et al. (2012) and applied to OSIRIS measurements, with a few minor modifications. The unnormalized measurement vector is given by,

$$\tilde{y}_{jk} = \log\left[I_j(h_k, 745.67\,\mathrm{nm})\right] - \log I_{j,\mathrm{ray}}(h_k, 745.67),. \quad (5)$$

~~where I_{ray} is a radiative transfer calculation performed with no aerosols in the atmosphere (pure Rayleigh background).~~ Similar to the ozone retrieval the measurement vector is normalized by a high altitude measurement. The altitude of normalization is chosen following the technique described by Bourassa et al. (2012)~~where the~~ , which first involves normalization the above measurement vector by a radiative transfer calculation done with no aerosols in the atmosphere (pure Rayleigh background). The normalization altitude is then adjusted on an image by image basis to minimize effects of stray light. Adjusting the normalization altitude on an image by image basis can cause sharp jumps in the normalization altitude across the orbital direction. It is currently unclear whether or not this adjustment is ideal for a two-dimensional retrieval, however as the aerosol retrieval is done primarily as a first order correction for the ozone retrieval this has not been investigated in detail.

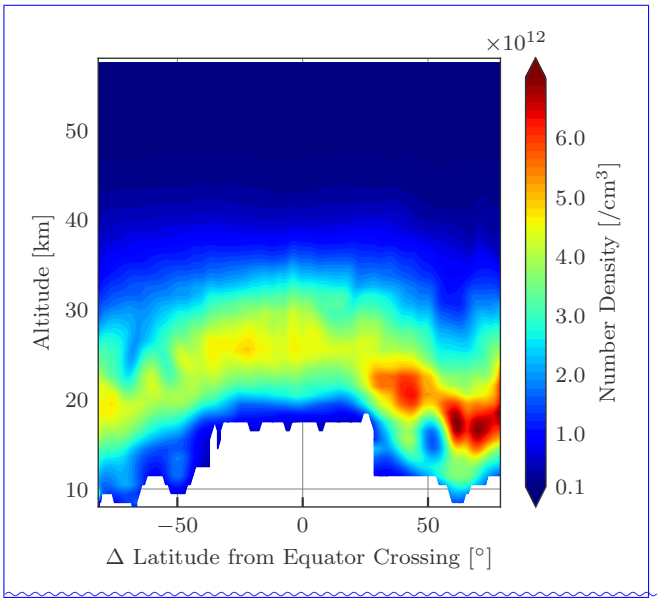

Figure 5. Retrieved ozone number density for OMPS-LP orbit 27695 (March 2nd, 2017, 10:30 AM UTC at equator crossing).

The measurement vector described here differs from that of Bourassa et al. (2012) in that there is no normalization relative to a shorter wavelength (470 nm for the OSIRIS retrieval). The short wavelength normalization was included to reduce the dependence of knowledge of the background Rayleigh atmosphere. However issues were encountered in that the short wavelength would often be measured on a different gain setting than the longer wavelength, introducing artifacts in the retrieval (see Jaross et al., 2014, for more information on the gain settings of OMPS-LP). Since there exist many limb scatter aerosol retrieval algorithms that operate without a short wavelength normalization Rault and Spurr (2010, e.g.) for simplicity we have opted to remove it. Stratospheric aerosols in the retrieval are assumed to consist of liquid H_2SO_4 spherical droplets following a log-normal particle size distribution with a median radius of 80 nm and a mode width of 1.6. The phase function ~~is~~ and cross sections are calculated using a standard Mie scattering code (Wiscombe, 1980), using the index of refraction from Palmer and Williams (1975).

2.8.2 Albedo

The forward model assumes a Lambertian reflecting surface parameterized by the albedo, the ratio of outgoing to incoming radiance. Typically this quantity does not physically represent actual reflectance from the surface of the Earth, but is used as an approximation for all upwelling from the troposphere. It is important to retrieve the albedo as many wavelengths used in the ozone retrieval are affected by ~~atmospheric upwelling~~ upwelling radiation.

While ~~the albedo is handled in a two-dimensional sense in~~ albedo in the forward model is allowed to vary in the horizontal direction, several assumptions are made which make the albedo retrieval similar to a set of independent one dimensional retrievals. Furthermore the albedo retrieval is not done under the Rodgers approach described earlier, and instead follows the

approach of Bourassa et al. (2007). We define the albedo state vector x_{alb} as the albedo on the surface of the Earth assuming a Lambertian surface at a set of latitudes and longitudes defined by the 40 km tangent point of each image. Therefore the state vector is the same length as the number of images used in the retrieval.

The albedo is iteratively updated with the equation,

$$x^{i+1}_{\text{alb},j} = x^{i}_{\text{alb},j} \frac{I_{j,\text{meas}}(40\,\text{km}, 745.67\,\text{nm})}{I_{j,\text{mod}}(40\,\text{km}, 745.67\,\text{nm})}. \tag{6}$$

The measurement vector uses the same wavelength as the aerosol retrieval since their effects tend to be coupled together. The retrieval is one-dimensional in the sense that, at least for one specific iteration, each image is allowed to only affect one element of the albedo state vector. However the forward modeled radiance is calculated using the two-dimensional albedo field, which allows images to couple to other elements of the state vector over the course of multiple iterations.

The spectral dependence of the albedo is neglected in the present retrieval. Loughman et al. (2005) estimates that neglecting realistic surface types (such as desert or savannah type surfaces) can cause systematic biases of up to 4% at 10 km for typical ozone retrievals. However these results are likely worst case estimates, as realistic tropospheric upwelling is expected to be more spectrally diffuse than a clear surface.

2.9 Regularization

The retrieval uses an ad-hoc Tikhonov style (Tikhonov, 1943) second derivative constraint applied only in the horizontal direction of the retrieval grid. The regularization matrix takes the form,

$$R = \alpha \begin{pmatrix} -\frac{1}{4} & \mathbf{0} & \frac{1}{2} & \mathbf{0} & -\frac{1}{4} & 0 & 0 & \dots \\ 0 & -\frac{1}{4} & \mathbf{0} & \frac{1}{2} & \mathbf{0} & -\frac{1}{4} & 0 & \dots \\ 0 & 0 & -\frac{1}{4} & \mathbf{0} & \frac{1}{2} & \mathbf{0} & -\frac{1}{4} & \dots \\ \vdots & \vdots & \vdots & \vdots & \vdots & \vdots & \vdots & \ddots \end{pmatrix}, \tag{7}$$

where α is a constant scaling factor used to control the amount of regularization and $\mathbf{0}$ indicates a number of zeros equal to the number of altitude grid points minus one. The value of α is chosen to control the horizontal resolution of the retrieved species, e.g. the value for ozone is 40 resulting in a $300 - 400$ km horizontal resolution (see Sec. 4). The apriori state vector of Eq. (2) is chosen to be 0. As the regularization matrix used only applies in the horizontal direction, the horizontally integrated vertical resolution of the retrieved profiles matches the vertical resolution of the retrieval grid.

It should be noted that even though we apply no constraints in the vertical direction, the retrieval software is capable of doing so. While the above discussion treats the horizontal and vertical dimensions of the grid as separate entities, the retrieval vertical and horizontal resolutions are inherently coupled together. A lower resolution horizontal grid allows for a higher resolution vertical grid, keeping the total information content relatively constant, and vice-versa. We make no claims on what is the optimal relationship between these two resolutions, and it is something that we are actively investigating. It is important to mention that a one-dimensional retrieval makes the trade-off decision for you, allowing control of only the vertical constraint.

The effects of a one-dimensional retrieval on horizontal resolution has been studied for the Michelson Interferometer for Passive Atmospheric Sounding by von Clarmann et al. (2008).

3 Pointing correction

Accurate and stable pointing knowledge is of particular importance for limb-scatter measurements as it is typically not possible to simultaneously measure pressure. Moy et al. (2017) provides a detailed characterization of the OMPS-LP pointing errors, however many of these corrections have ~~not~~ only been applied to the v2.5 L1G product, and not the v2.0–2.4 L1G product used in this study. Therefore for the current version of the retrieval a separate pointing analysis has been performed.

We apply the Rayleigh Scattering Attitude Sensor (RSAS) (Janz et al., 1996) to the OMPS-LP measurements. The ratio of the measured radiance at 40 km and 20 km near 350 nm is compared to the calculated radiance. At 40 km the radiance is sensitive to tangent altitude changes, while at 20 km the radiance is not very sensitive since the line of sight path has become optically thick. Based on the difference between the measured and modeled ratios it is possible to calculate an effective tangent altitude offset. The RSAS technique is sensitive to both ~~atmospheric upwelling~~ upwelling radiation and stratospheric aerosol loading which makes it difficult to apply at low solar zenith angles and in forward scatter conditions respectively.

To minimize the effects of both ~~atmospheric upwelling~~ upwelling radiation and stratospheric aerosols we only use measurements with solar zenith angle between 70° and 50° with solar scattering angles greater than 90°. Measurements satisfying similar criteria have recently been successfully used to apply an RSAS pointing correction to OSIRIS retrievals by Bourassa et al. (2017). While measurements with a solar zenith angle greater than 70° would have even less upwelling, it is more challenging to accurately model the multiple scatter component of the radiance. Cutoffs greater than 50° were not found to affect the results, 50° was chosen to maximize the number of measurements. The altitude offsets were daily averaged and shown in Fig. 6. Offsets range from approximately 400 m to 0 m with a clear seasonal cycle, in April 2013 there is noticeable $\sim$100 m drop due to a known star tracker adjustment. Being able to clearly observe the star tracker adjustment provides confidence that at least on a relative scale we are able to detect pointing shifts with the RSAS method.

It is currently unknown whether or not the seasonal structure represents a true pointing shift or if it is an artifact of the RSAS method–perhaps due to the average latitude of the measurements also varying seasonally and changing cloud cover. We do not detect any significant pointing drift greater than $\pm$100 m, however later years are affected by stratospheric aerosols from Kelud and Calbuco which may skew the RSAS technique. Preliminary validation efforts have revealed that, on average, there is likely an absolute pointing error present in the OMPS-LP measurements. To calculate the applied pointing correction (solid line in Fig. 6) we take an average value both before and after the star tracker adjustment. All ozone profiles are shifted downwards by this amount after the retrieval has been performed. It should be noted that this applied pointing correction is by intention simple. A future version of the data product will examine the pointing in more depth, and apply the correction to the instrument lines of sight rather than post shifting the retrieved profile.

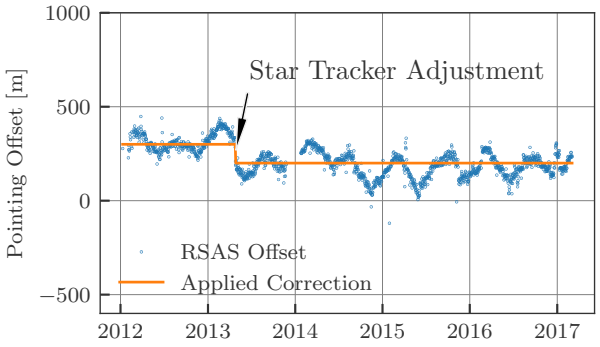

Figure 6. Daily averaged pointing offsets calculated with the RSAS technique. The orange line shows the applied pointing correction for v1.0.2 of the retrieved data product.

4 Error analysis and resolution

Both the random and systematic error components of a limb scatter ozone retrieval algorithm for a similar, but one-dimensional, retrieval have been studied in Loughman et al. (2005). Applying the conclusions of Loughman et al. (2005) to our retrieval algorithm suggests that the dominant sources of random error are pointing knowledge and the error due to measurement noise. Rault and Loughman (2013) have also presented similar findings for a one-dimensional retrieval algorithm applied to OMPS-LP, and in particular showed that the error due to measurement noise is representative of the total random error budget. We will not repeat these analyses here, rather we will simply present the technique used to calculate the reported error estimate for each orbit.

Under the Rodgers framework the gain matrix, $\hat{\mathbf{G}}$, is given by,

$$\hat{\mathbf{G}} = (\hat{\mathbf{K}}^T \mathbf{S}_\epsilon^{-1} \hat{\mathbf{K}} + \mathbf{R}^T \mathbf{R})^{-1} \hat{\mathbf{K}}^T \mathbf{S}_\epsilon^{-1}, \tag{8}$$

and the averaging kernel,

$$\mathbf{A} = \hat{\mathbf{G}}\hat{\mathbf{K}}, \tag{9}$$

where the hats indicate that the solution has converged. The solution covariance due to measurement noise only can also be estimated as,

$$\hat{\mathbf{S}}_{\text{noise}} = \hat{\mathbf{G}} \mathbf{S}_\epsilon \hat{\mathbf{G}}^T. \tag{10}$$

In the current version of the retrieval only the solution covariance due to measurement noise is reported. For the purposes of the precision estimate we assume that the measurement covariance is diagonal, with the radiance measurements having a signal to noise ratio of 100, an upper bound on the error estimate taken from Jaross et al. (2014). Only the diagonal elements of the solution covariance are used for the error estimate. Since the state vector is the logarithm of number density, the precision estimate in logarithmic space is propagated to linear space for the reported precision estimate.

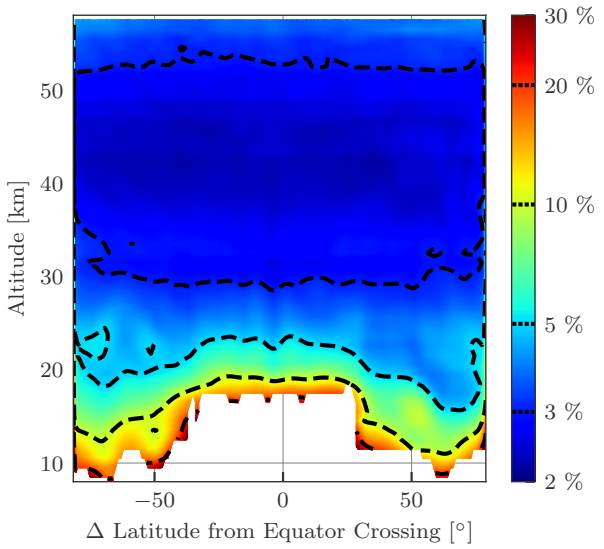

Figure 7. Precision estimate for ozone in percent for OMPS-LP orbit 27695 (March 2nd, 2017, 10:30 AM UTC at equator crossing). Contour levels are indicated by dashed lines on the colorbar. The corresponding retrieved ozone profiles are shown in Fig. 5.

Figure 7 shows an example precision estimate for OMPS-LP orbit 27695 (March 2nd, 2017, 10:30 AM UTC at equator crossing). Precision estimates are in the range 2–5% for the majority of the middle and upper stratosphere. In the lower stratosphere precision is ∼10% increasing to 30% near the tropopause. Various edge effects of the retrieval are also visible, most noticeably the increase in error at the beginning and end of the orbit ~~but~~ and near where the ~~tropopause lowers~~ lower bound of the retrieval changes (due to the lowering tropopause) at mid-latitudes. These are expected effects, edges of the retrieval grid inherently have less measurements contributing to them, increasing the expected noise. The estimate precision varies only slightly between orbits, and the values stated above are generally valid for the entire dataset.

The resolution of the retrieval is found by analyzing the retrieval averaging kernels. As the retrieval is two-dimensional, each row of the averaging kernel contains both vertical and horizontal components. Since the regularization term (Eq. (7)) contains no vertical information, it can be shown that the horizontally summed averaging kernel (i.e., the vertical averaging kernel) is the identity matrix. This has also been verified by calculating the vertical averaging kernel for a set of OMPS-LP orbits, which were all found to be identically unity. Considering the vertical averaging ~~kernels~~ kernel contain little information, we will focus on the vertically integrated, or horizontal, averaging ~~kernels~~kernel.

Figure 8 shows the rows of the horizontal averaging kernel for ~~orbit 27695~~ two orbits in different seasons at 0° N and 55° N. In both cases the horizontal FWHM is smallest near 40 km with values of $\sim 250\,\mathrm{km}$. For the majority of the altitude range the FWHM is less than $400\,\mathrm{km}$, with the exception of the region near the tropopause where it can increase to $500\,\mathrm{km}$. Only minor differences in the FWHM are seen between the tropical and mid-latitude averaging ~~kernels~~kernel rows, with the majority of the differences occuring near the lower bound of the retrieval. Averaging kernels are not stored for every orbit due to size

constraints, however it was found that ~~there was almost no variation~~ deviations from orbit to orbit ~~and the ones shown here~~ are small enough that the above resolution estimates are representative for the entire dataset.

As previously stated, the vertical averaging kernels are identity, suggesting that the vertical resolution of the retrieval is 1 km, the same as the retrieval grid. However, the instrumental vertical field of view ($\sim$ 1.5 km, see Jaross et al., 2014) is neglected in the retrieval process, treating each measurement with a single line of sight. Therefore we estimate the vertical resolution of the retrieved profiles to be 1–2 km. It is intended to investigate the vertical resolution in more detail for future versions of the retrieval.

5 Preliminary results

5.1 Simulations on the edge of the polar vortex

To test the retrieval method, a one-dimensional retrieval method that assumes horizontal homogeneity has also been developed to compare against. The one-dimensional retrieval has been designed to be as similar to the two-dimensional retrieval as possible. The measurement vectors for ozone, albedo, and stratospheric aerosol are the same as those ~~those~~ for the two-dimensional retrieval, with the only difference being that the number of images used is one instead of an entire orbit. The state vector is modified to be one-dimensional in altitude, representing a horizontal homegenous atmosphere with 1 km vertical spacing. As the Tikhonov regularization is only applied in the horizontal direction for the two-dimensional retrieval, no regularization is used in the one-dimensional retrieval. The same iterative procedure is also used for the one-dimensional retrieval.

To test the ability of the two-dimensional retrieval to resolve horizontal gradients in the ozone field, simulated retrievals have been performed. For the simulations, measurements from a full OMPS-LP orbit are simulated using a two-dimensional ozone field. The resulting radiances are then used in both the one and two dimensional retrievals. To isolate the effects of horizonal ozone gradients, the input aerosol and albedo fields are assumed to be known and horizontally homogenous.

Figure 9 shows the results of the simulated retrieval for OMPS-LP orbit 20567. Qualitatively there is good agreement between the one and two dimensional retrievals and the true ozone field, providing confidence in both methods. The two-dimensional retrieval agrees to better than 5% with the true ozone profile almost everywhere, with a few exceptions below 20 km. Looking at the 15.5 km slice of the retrieval (top right panel of Fig. 9) it can be seen near 50° S that the two-dimensional retrieval smooths out some of the fine oscillatory structure of the true profile, which is expected from the form of the averaging kernel. That being said, the two-dimensional retrieval captures the large ozone gradient in the 75° S to 60° region very well.

Overestimation by the one-dimensional retrieval can be seen in the 75° S to 60° region, 10–20 km region. The 15.5 km slice reveals that the one-dimensional retrieval assigns the horizontal gradient to the wrong location, leading the true profile by $\sim 2°$. Consistent overestimation by the one-dimensional retrieval is what would be expected by the measurement geometry and input ozone field. As OMPS-LP looks backward in the orbital plane, measurements near the edge of the polar vortex consistently look through high ozone values into lower ozone values. For limb scatter measurements ozone sensitivity is larger on the instrument side of the line of sight (for an indepth discussion of this effect see Zawada et al., 2017), the high ozone values near OMPS-LP are incorrectly assigned to tangent points inside or near the vortex.

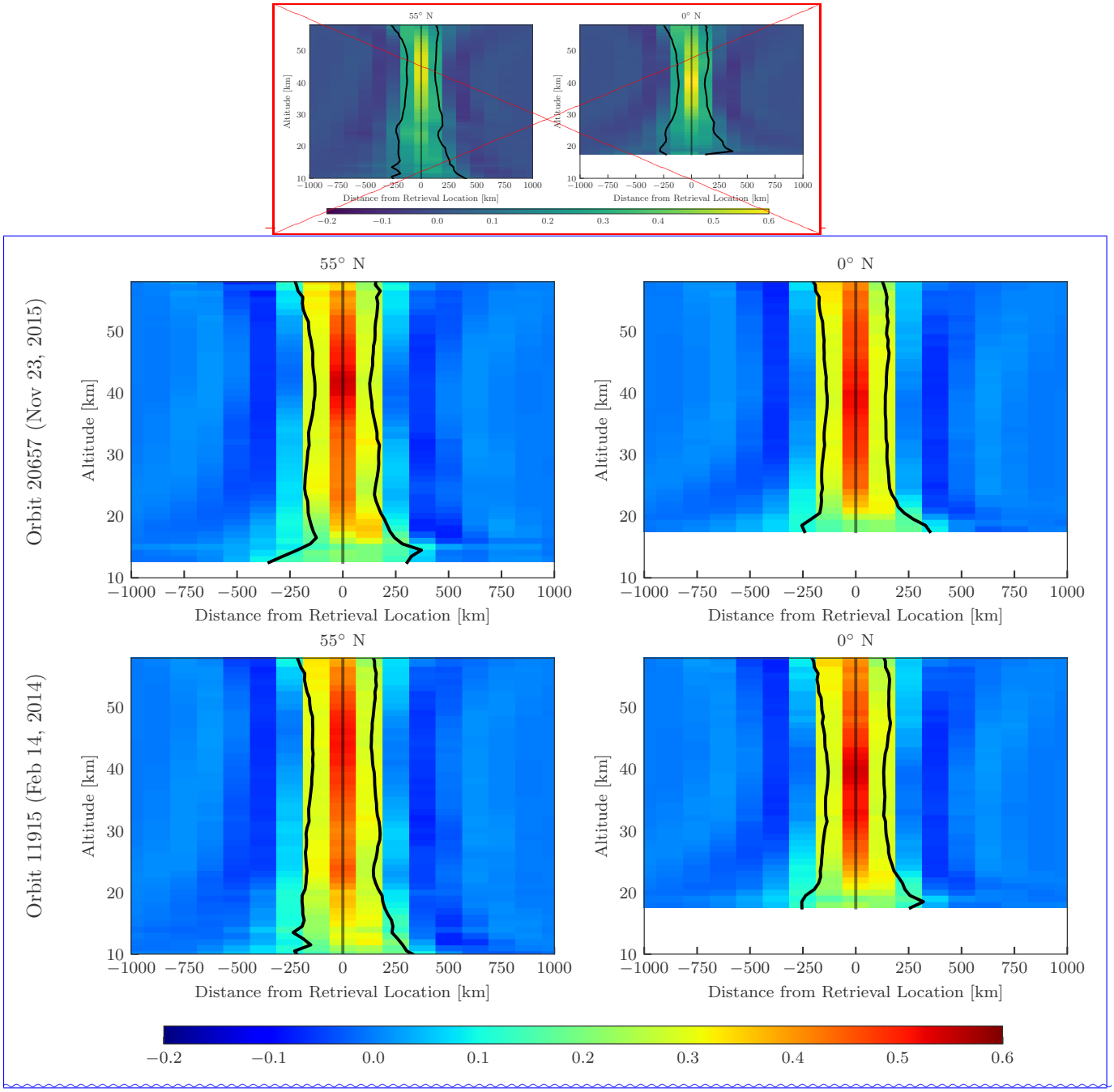

Figure 8. Horizontal averaging kernels from OMPS-LP orbit ~~27695~~ 20657 (~~March 2nd~~October 23rd, ~~2017~~2015, ~~10~~8:~~30~~50 AM UTC at equator crossing) and OMPS-LP orbit 11915 (February 14th, 2014, 4:35 AM UTC at equator crossing) for 55° N (left panel) and 0° N (right panel). Data is masked below the lowest retrieval altitude. Vertical black lines show the full width at half maximum boundaries, while the vertical gray line indicates the location of the retrieval. Distance from the retrieval location is defined as negative towards the start of the orbit in the southern hemisphere, and positive towards the end of the orbit in the northern hemisphere.

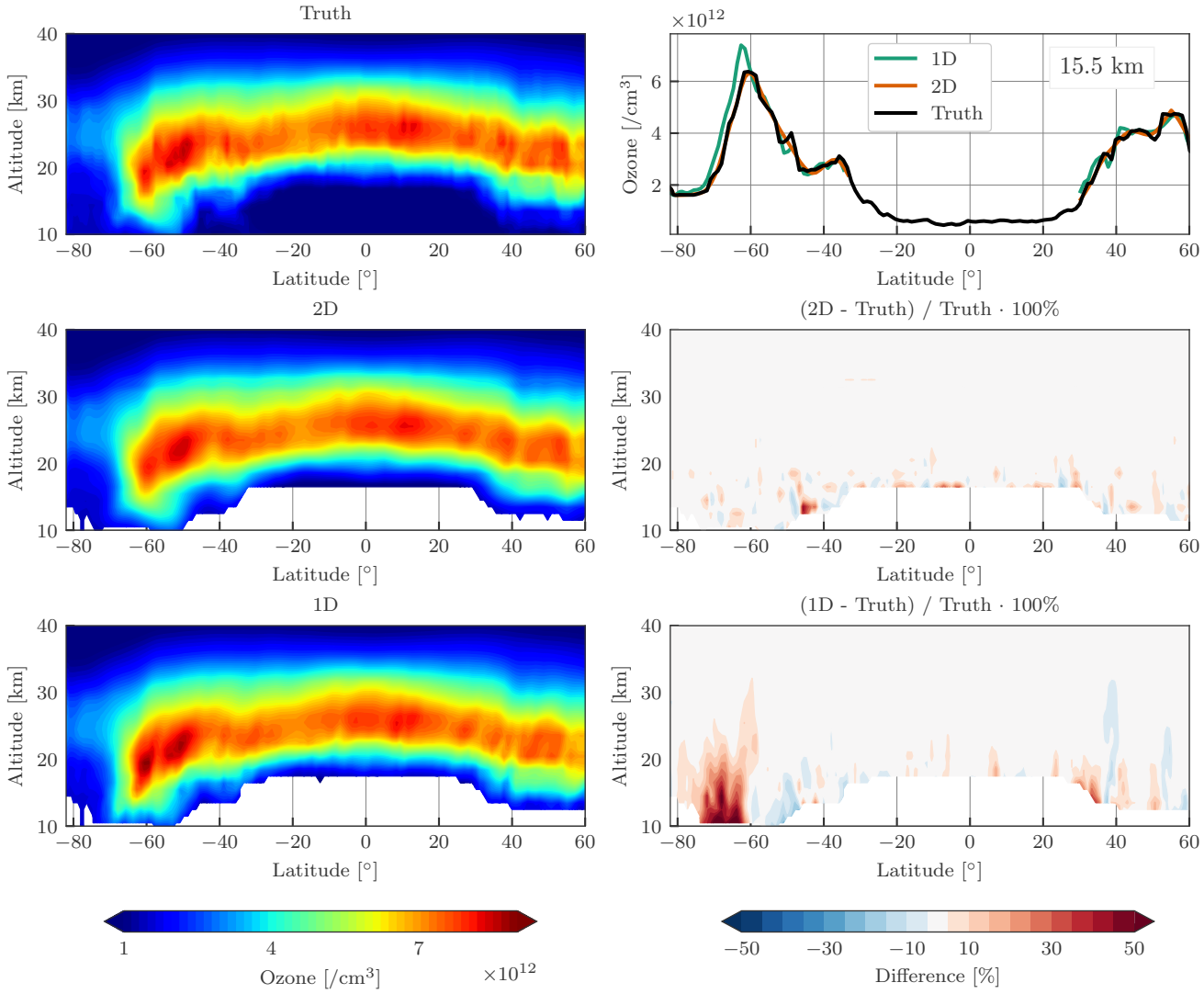

Figure 9. Simulated retrieval results for OMPS-LP orbit 20657 ~~near the polar vortex~~(October 23rd, 2015, 8:50 AM UTC at equator crossing). The left column shows the true ozone field (top), tomographically retrieved ozone (middle), and the one-dimensionally retrieved ozone (bottom). The right column contains a horizontal slice of the retrieved ozone at 15.5 km (top), the percent difference between the tomographic retrieval and the truth (middle), and the percent difference between the one-dimensionally retrieved ozone and the truth (bottom). For the percent difference panels contours are shown every ±5%.

5.2 ~~Example retrieved orbit with OMPS-LP~~

~~Figure 5 shows the retrieved ozone number density for~~ To assess the impact of viewing geometry on the retrieval a second simulation has been performed with a large horizontal ozone gradient present in the northern hemisphere. For this simulation the geometry from OMPS-LP orbit ~~27695. Several low ozone filaments above the ozone layer are visible in both the southern hemisphere and northern hemisphere tropics/mid-latitudes. In the northern hemisphere a low pocket of ozone can be seen below and intruding into the ozone layer.~~

~~Processing of this orbit took approximately 124 minutes using 8 threads on an i7-4770k cpu. There were 159 vertical images of radiance data input to the retrieval~~12300 (March 14th, ~~giving an approximate processing time of 47 seconds per vertical image.Thus performing the 2D retrieval is not onerous from a computational point of view, two machines of similar computational power are sufficient to keep up to date with routine processing~~2014) was used. The simulated ozone field was taken from March 14th, 2011 to obtain a realistic scenario with large polar ozone depletion. The results of the simulation are shown in Fig. 10.

The one-dimensional retrieval consistently underestimates the true ozone profile in the $60-70^{\circ}$ N region. In this gradient region looks through low ozone values into high ozone values, opposite of the prior simulation, thus underestimation is expected. As before, the one-dimensional retrieval leads the true profile, which can be seen in the 17.5 km slice (top right panel of Fig. 10). The magnitude of the underestimation (10–20%) is less than the overestimation of the prior simulation (50%), primarily because the gradient is weaker and does not extend into the lower altitudes. The two-dimensional retrieval captures the structure of the gradient quite well, and as before, some horizontal smoothing errors on the order of 5–10% can be seen at altitudes below 20 km.

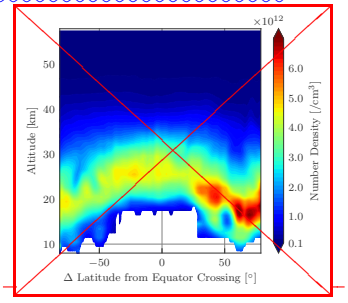

5.2 Monthly zonal mean anomalies

As a zeroth order valdiation effort monthly zonal mean relative ozone anomalies have been performed against the MLS v4.2 ozone measurements. The MLS retrievals (Livesey et al., 2006) native product is volume mixing ratio on pressure surfaces, for these comparisons we have converted MLS v4.2 measurements to number density on altitude levels using ERA-interim reanalysis (Dee et al., 2011). The MLS data has been screened according to the recommendations of Livesey et al. (2017). Figure 11 shows the result of these comparisons in the tropical 5° S to 5° N latitude bin. Qualitatively there is excellent agreement, the anomalous change in the QBO beginning at the end of 2015 can clearly be seen in both datasets. Quantitatively,

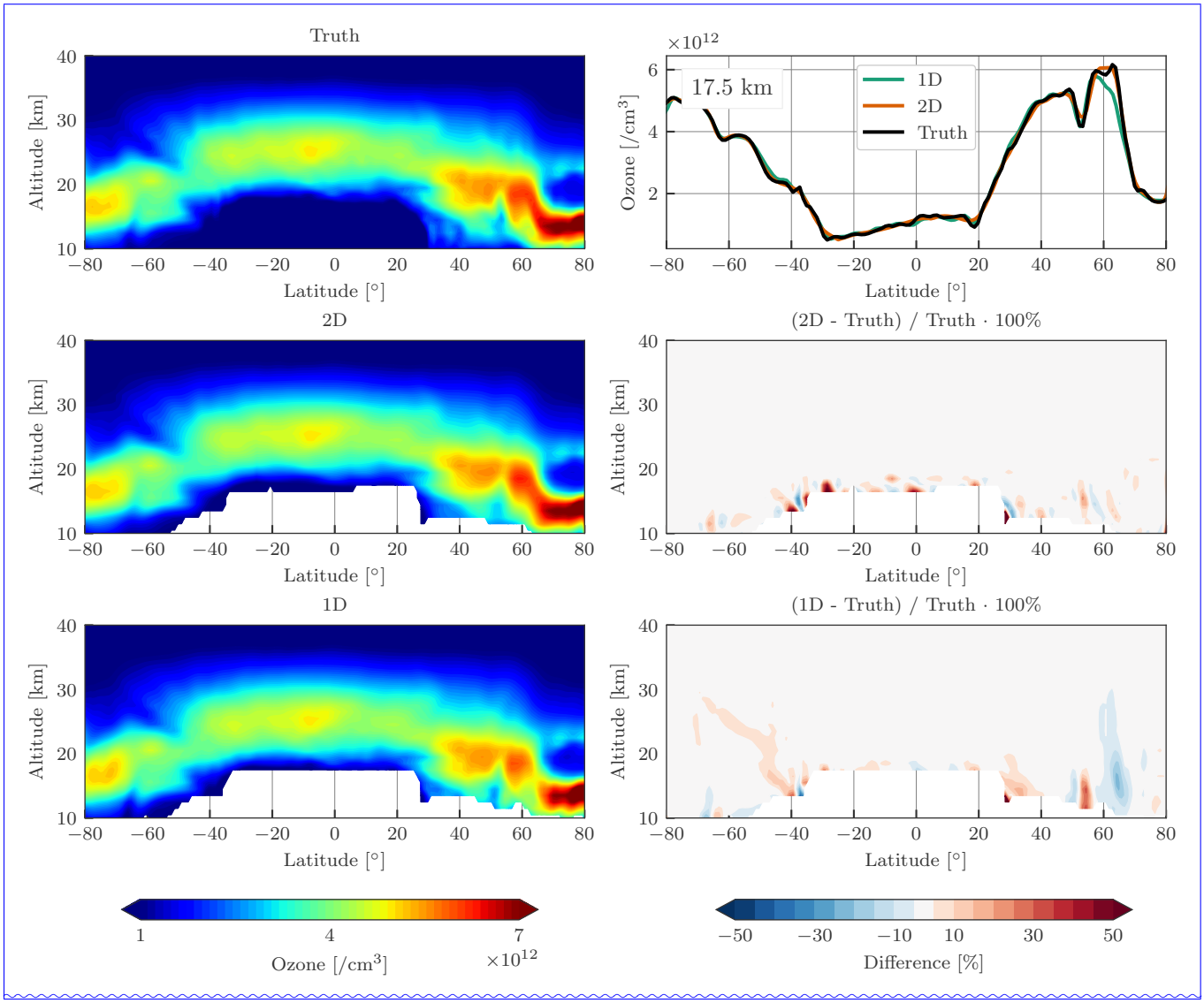

Figure 10. ~~Retrieved ozone number density~~ Same as Fig. 9 but for OMPS-LP orbit ~~27695 (March 2nd, 2017, 10:30 AM UTC at equator crossing).~~12300.

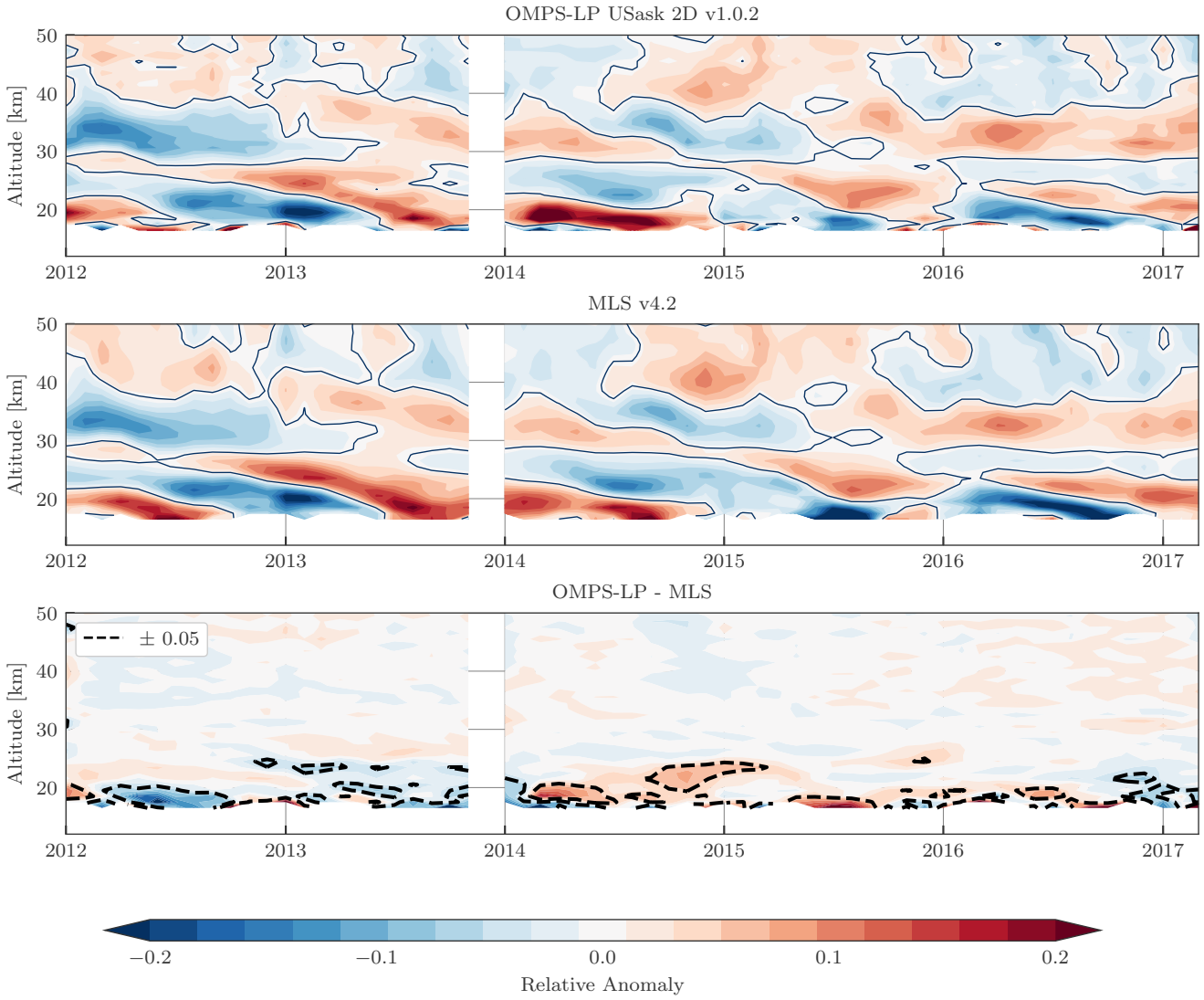

Figure 11. Monthly zonal mean ozone anomalies in the 5° S to 5° N bin for OMPS-LP (top), MLS v4.2 (middle), and their absolute difference (bottom). Anomalies are calculated relative to the common overlap period, and data is masked outside the common overlap period.

above 25 km observed differences in relative anomaly are less than 0.05 ($\sim$ 5% change in ozone) for all time periods. Below 25 km differences on the order of 0.1 are seen, which could be related to larger variability in the tropical UTLS.

5.3 Near perfect coincidences with MLS

MLS onboard Aura and OMPS-LP onboard Suomi-NPP are both in sun-synchronous orbit with similar inclination and local crossing times, however Suomi-NPP orbits near $\sim$ 800 km while Aura is at $\sim$ 700 km. The slight difference in orbital periods

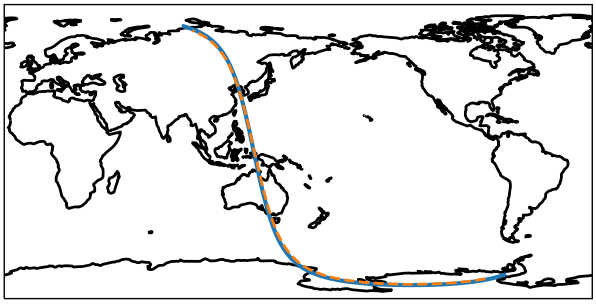

Figure 12. An example of near perfect coincident measurements from OMPS-LP and MLS. The dashed orange line shows the retrieval grid points for OMPS-LP orbit 11915 (February 14th, 2014, 4:35 AM UTC at equator crossing), while the blue line shows the retrieval locations for the near coincident MLS measurements. The time difference at the crossing point is ∼16 minutes.

causes the measurement ground tracks to drift relative to each other, with near perfect overlap, in both space and time, every 2–3 days. Figure 12 shows the measurement track of OMPS-LP orbit 11915 (February 14th, 2014, 4:35 AM UTC at equator crossing), also shown are the available measurements from MLS which are nearly perfect coincident to the OMPS-LP measurements. At the crossing point there is a time difference of 16 minutes, and the differences in longitude are less than 1° for the entire orbit track. It should be mentioned that sampling differences in latitude do not play a large factor as both the MLS and OMPS-LP retrievals are two-dimensional with the horizontal along-track resolution being poorer than the sampling frequency. For example, at 20 km, the OMPS-LP retrieval has a horizontal sampling of $\sim$ 125 km with an estimated horizontal resolution of 350 km while MLS v4.2 samples every ∼150 km with a horizontal resolution of 300 km (Livesey et al., 2017).

The MLS retrieval is also two-dimensional, and has similar along-track resolution to the two-dimensional OMPS-LP retrieval, thus we have not applied horizontal averaging kernels for these tests. To account for differences in vertical resolution the procedure recommended by Livesey et al. (2017) has been used. The OMPS-LP ~~data has been~~ data is degraded to the MLS pressure grid with a least squares fit, and then converted back to the altitude grid in a consistent fashion, however internal tests have shown that this makes negligable differences. A full validation of the dataset is intended for a forthcoming publication, however an initial validation check has been performed by examing near coincident orbits between Aura (MLS) and Suomi-NPP (OMPS-LP).

Figure 13 shows the retrieved ozone for OMPS-LP orbit 11915 (February 14th, 2014, 4:35 AM UTC at equator crossing) and coincident MLS measurements. Qualitatively there is excellent agreement between the two retrievals. A triple ozone peak at low altitudes is seen in both retrievals in the northern hemisphere, and both retrievals resolve a break in the ozone peak near $40^\circ S$. Some slight horizontal oscillations are observed ($\sim \pm 5\%$) in the USask OMPS-LP retrieval near the equator. The exact cause of the oscillations is currently unknown, but initial investigation suggests that it could be caused by the combination of cloud cover affecting the large amount of upwelling observed due to low solar zenith angles ($\sim 20^\circ$) seen in the tropics.

Quantitatively agreement between the two retrievals (bottom panel of Fig. 13) is better than 5% for the majority of the stratosphere. Differences greater than 10% are seen at the lowest altitudes of the retrieval grid, it is possible that these are

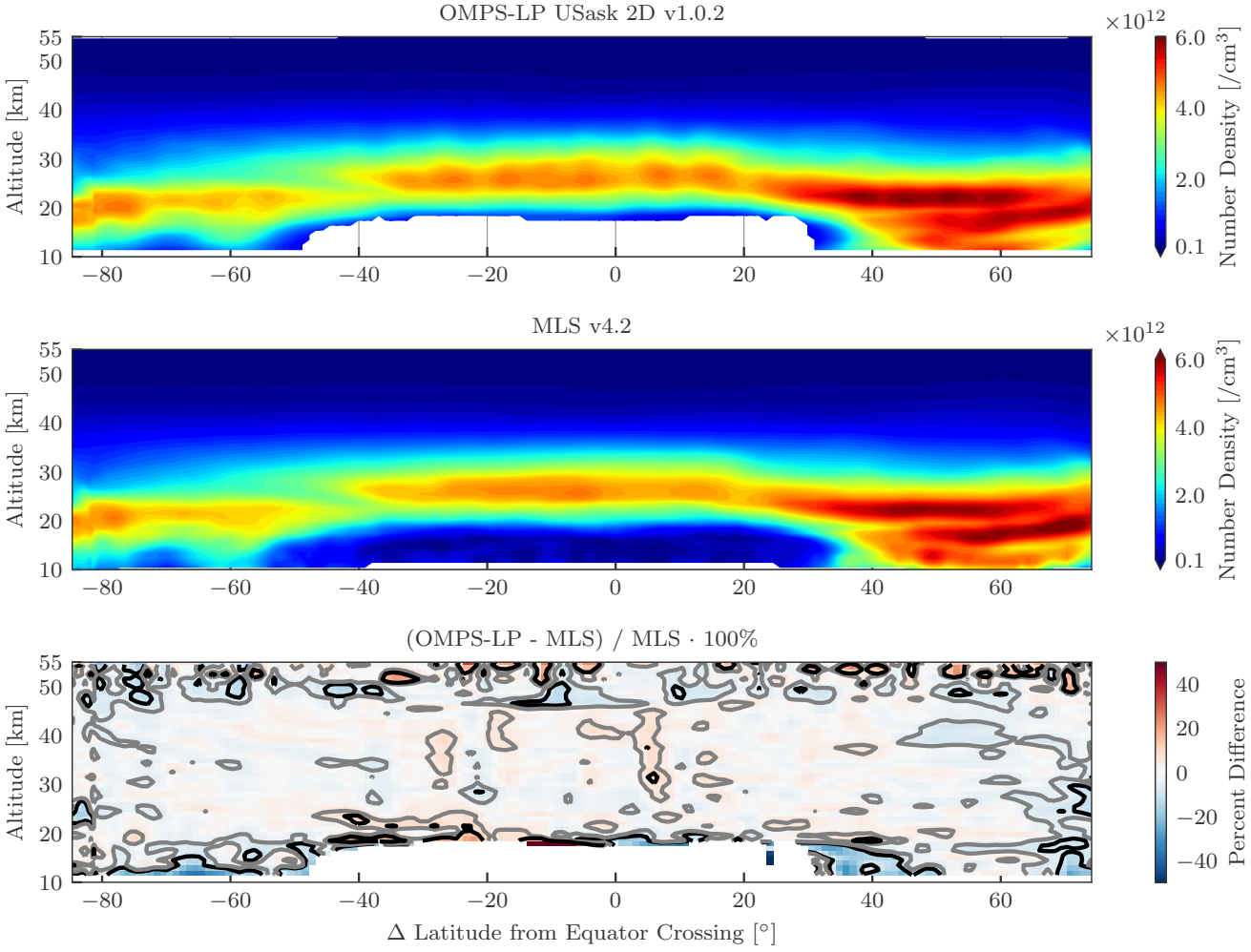

Figure 13. The top panel shows the retrieved ozone field for OMPS-LP orbit 11915 (February 14th, 2014, 4:35 AM UTC at equator crossing) from the USask 2D v1.0.2 retrieval, and the middle panel shows the corresponding coincident MLS v4.2 retrieved values for the coincident measurements shown in Fig. 12. The bottom panel shows the percent difference between the two, with gray and black contours indicating the $\pm 5\%$ and $\pm 10\%$ levels respectively.

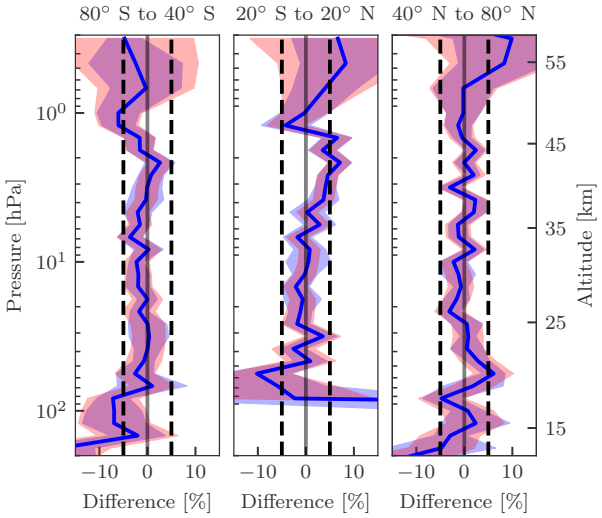

Figure 14. Mean differences ((OMPS-LP - MLS) / MLS · 100%) in three latitude bins for the comparison shown in Fig. 13. The shaded blue region shows the standard deviation of the differences, while the shaded red region is the predicted standard deviation using the precision estimate from both retrievals. Dashed vertical lines indicate the $\pm 5\%$ levels.

caused by the non-linearity involved in applying the pointing correction to the retrieved profile rather than the measurement tangent altitudes themselves. At the northern edge of the retrieval grid there are also differences on the order of $5-10\%$ which could be indicative of an edge effect in the two-dimensional retrieval. Above 45 km there is a large amount of variance observed, however this is reflected in the MLS precision estimate ($\sim 20\%$ at 0.5 hPa).

Figure 14 compares the same orbit in three latitude bins, 80° S to 40° S, 20° S to 20° N, and 40° N to 80° N. Also shown in Fig. 14 with the observed standard deviation, providing confidence in the supplied precision values for both OMPS-LP and MLS. However since each bin contains only roughly 30 measurements, these statistics should only be viewed as a rough qualitative estimate. In-depth studies using a large number of coincident orbits are planned for future validation efforts.

Lastly, results are shown for OMPS-LP orbit 20657 (October 23rd, 2015, 8:50 AM UTC at equator crossing) are shown which are also nearly perfectly coincident to measurements from MLS. For this orbit we also apply the one-dimensional retrieval described in Sec. 5.1, and the retrieval results are shown in Fig. 15. Similar to the previous orbit, agreement in the middle stratosphere is typically better than 5% between MLS and the two-dimensional retrieval. The one-dimensional retrieval also agrees favorably with MLS in the middle stratosphere. Inside the vortex there is larger disagreement, however this is expected due to the low absolute ozone values and the inherent variance of the retrievals.

Highlighted in Fig. 15 (dashed lines) is the 60° S to 75° S, 10–20 km region, which is the region where the one-dimensional retrieval performed poorly in the simulations of Sec. 5.1. In this region the two-dimensional retrieval agrees better with MLS than the one-dimensional retrieval, with the one-dimensional retrieval consistently overestimating the ozone values. The 15.5 km slice (top right panel of Fig. 15) shows the one-dimensional retrieval leading both MLS and the two-dimensional

retrieval, which is consistent with the prior simulation results. If we interpret the difference between the profiles at 15.5 km entirely as a latitudinal offset then the difference between the two-dimensional retrieval and MLS is ∼0.5° while the difference between the one-dimensional retrieval and MLS is ∼2° at 65° S.

6 Conclusions

A two-dimensional retrieval algorithm which directly accounts for atmospheric variations in the along orbital track dimension has been developed for use with limb scatter measurements from OMPS-LP. The retrieval algorithm combines all measurements from the sunlit portion of the orbit and simultaneously fits the full ozone profile for the ~~entire orbit~~ portion of the orbit with solar zenith angle less than 88°. The vertical resolution of the retrieved profiles is estimated to be 1–2 km while the along-track resolution is controlled with a Tikhonov type second squared difference constraint, and is typically 300–400 km for retrievals from OMPS-LP. The estimated precision of the retrieved ozone product is 2–5% for the middle and upper stratosphere, with values increasing to 30% just above the tropopause. Simulated retrievals were shown indicating that the retrieval is working as expected, and offers improvement over traditional one-dimensional retrievals in areas of large horizontal gradients.

The retrieval algorithm has been applied to all measurements from the center slit of OMPS-LP from early 2012 to present to create a multi-year near-global ozone time-series. Tropical ozone anomalies from the dataset agree well with those from MLS v4.2, with differences greater than 5% of the ozone mean value only observed below 25 km.

A preliminary validation effort is presented comparing ~~one orbit~~ two orbits of measurements to coincident measurements from MLS. These measurements are near perfectly coincident with time differences of less than 20 minutes and longitude differences of less than 1°. For the majority of the stratosphere differences are less than 5%, larger differences are seen at the edges of the retrieval grid. Qualitatively the precision estimate matches the observed scatter seen in the differences. Coincident comparisons during the 2015 ozone hole indicates that the two-dimensional retrieval and MLS agree qualitatively well at the edge of the polar vortex, whereas a ~~tradiational~~ traditional one-dimensional retrieval is shown to systematically overestimate in this area.

7 Data availability

The USask OMPS-LP v1.0.2 2D dataset is available in HARMOZ format (Sofieva et al., 2013) from the Odin-OSIRIS FTP server (see http://odin-osiris.usask.ca/?q=node/280).

Competing interests. The authors declare that they have no conflict of interest.

Acknowledgements. This work was partially funded by the Canadian Space Agency, the Natural Sciences and Engineering Research Council of Canada, Science Systems and Applications, Inc., and the National Aeronautics and Space Administration's Goddard Space Flight Center. We would also like to thank the OMPS-LP team for assistance and for providing a high quality L1 data product.

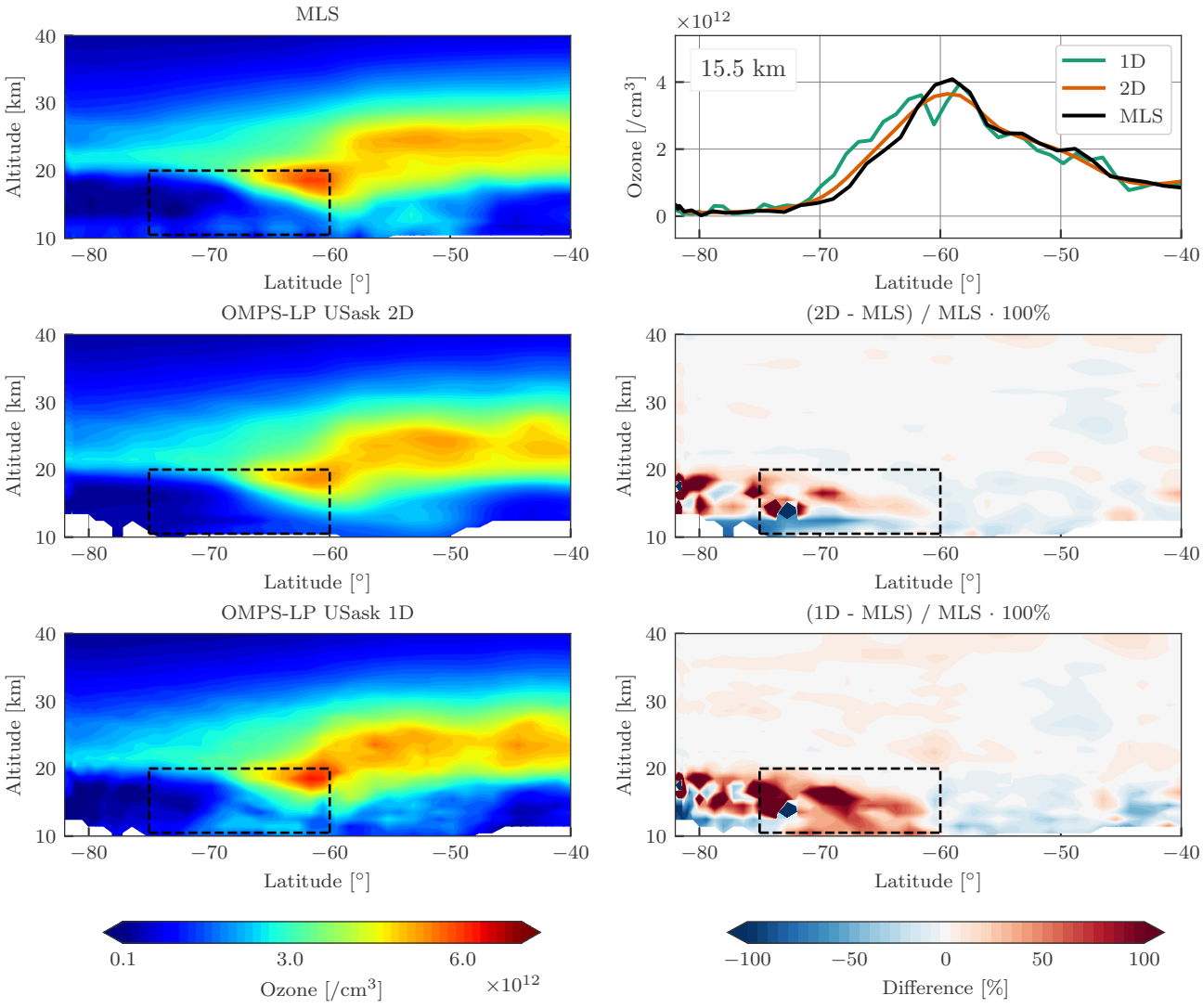

Figure 15. Retrieval results for OMPS-LP orbit 20657 (October 23rd, 2015, 8:50 AM UTC at equator crossing) near the polar vortex. The left column shows the coincident MLS v4.2 ozone (top), tomographically retrieved ozone (middle), and the one-dimensionally retrieved ozone (bottom). The right column contains a horizontal slice of the retrieved ozone at 15.5 km (top), the percent difference between the tomographic retrieval and MLS (middle), and the percent difference between the one-dimensionally retrieved ozone and MLS (bottom). For the percent difference panels contours are shown every ±5%. The dashed black box indicates the area in which the two-dimensional retrieval is expected to show improvement based upon the simulations of Sec. 5.1.

References

Bourassa, A. E., Degenstein, D. A., Gattinger, R. L., and Llewellyn, E. J.: Stratospheric aerosol retrieval with optical spectrograph and infrared imaging system limb scatter measurements, Journal of Geophysical Research, 112, D10 217, doi:10.1029/2006JD008079, 2007.

Bourassa, A. E., Degenstein, D. A., and Llewellyn, E. J.: SASKTRAN: A spherical geometry radiative transfer code for efficient estimation of limb scattered sunlight, Journal of Quantitative Spectroscopy and Radiative Transfer, 109, 52–73, doi:10.1016/j.jqsrt.2007.07.007, 2008.

Bourassa, A. E., Rieger, L. A., Lloyd, N. D., and Degenstein, D. A.: Odin-OSIRIS stratospheric aerosol data product and SAGE III intercomparison, Atmospheric Chemistry and Physics, 12, 605–614, doi:10.5194/acp-12-605-2012, http://www.atmos-chem-phys.net/12/605/2012/, 2012.

Bourassa, A. E., Roth, C. Z., Zawada, D. J., Rieger, L. A., McLinden, C. A., and Degenstein, D. A.: Drift corrected Odin-OSIRIS ozone product: algorithm and updated stratospheric ozone trends, Atmospheric Measurement Techniques Discussions, 2017, 1–16, doi:10.5194/amt-2017-229, https://www.atmos-meas-tech-discuss.net/amt-2017-229/, 2017.

Bovensmann, H.: SCIAMACHY: Mission objectives and measurement modes, Journal of the atmospheric sciences, pp. 127–150, 1999.

Brion, J., Chakir, A., Daumont, D., Malicet, J., and Parisse, C.: High-resolution laboratory absorption cross section of O3. Temperature effect, Chemical physics letters, 213, 610–612, 1993.

Carlotti, M., Brizzi, G., Papandrea, E., Prevedelli, M., Ridolfi, M., Dinelli, B. M., and Magnani, L.: GMTR : Two-dimensional geo-fit multitarget retrieval model for Michelson Interferometer for Passive Atmospheric Sounding / Environmental Satellite observations, Appl. Opt., 45, 716–727, doi:10.1364/AO.45.000716, https://www.osapublishing.org/ao/abstract.cfm?uri=ao-45-4-716, 2006.

Daumont, D., Brion, J., Charbonnier, J., and Malicet, J.: Ozone UV spectroscopy I: Absorption cross-sections at room temperature, Journal of Atmospheric Chemistry, 15, 145–155, 1992.

Dee, D. P., Uppala, S. M., Simmons, A. J., Berrisford, P., Poli, P., Kobayashi, S., Andrae, U., Balmaseda, M. A., Balsamo, G., Bauer, P., Bechtold, P., Beljaars, A. C. M., van de Berg, L., Bidlot, J., Bormann, N., Delsol, C., Dragani, R., Fuentes, M., Geer, A. J., Haimberger, L., Healy, S. B., Hersbach, H., Hólm, E. V., Isaksen, L., Kållberg, P., Köhler, M., Matricardi, M., Mcnally, A. P., Monge-Sanz, B. M., Morcrette, J. J., Park, B. K., Peubey, C., de Rosnay, P., Tavolato, C., Thépaut, J. N., and Vitart, F.: The ERA-Interim reanalysis: Configuration and performance of the data assimilation system, Quarterly Journal of the Royal Meteorological Society, 137, 553–597, doi:10.1002/qj.828, http://doi.wiley.com/10.1002/qj.828, 2011.

Degenstein, D. A., Llewellyn, E. J., and Lloyd, N. D.: Volume emission rate tomography from a satellite platform, Applied optics, 42, 1441–1450, 2003.

Degenstein, D. A., Llewellyn, E. J., and Lloyd, N. D.: Tomographic retrieval of the oxygen infrared atmospheric band with the OSIRIS infrared imager, Canadian Journal of Physics, 82, 501–515, doi:10.1139/p04-024, http://www.nrcresearchpress.com/doi/abs/10.1139/p04-024, 2004.

Degenstein, D. A., Bourassa, A. E., Roth, C. Z., and Llewellyn, E. J.: Limb scatter ozone retrieval from 10 to 60 km using a multiplicative algebraic reconstruction technique, Atmospheric Chemistry and Physics, 9, 6521–6529, doi:10.5194/acp-9-6521-2009, 2009.

Flittner, D. E., Bhartia, P. K., and Herman, B. M.: O3 profiles retrieved from limb scatter measurements: Theory, Geophysical Research Letters, 27, 2601–2604, doi:10.1029/1999GL011343, 2000.

Flynn, L. E., Seftor, C. J., Larsen, J. C., and Xu, P.: The ozone mapping and profiler suite, in: Earth science satellite remote sensing, pp. 279–296, Springer, 2006.

Janz, S. J., Hilsenrath, E., Flittner, D. E., and Heath, D. F.: Rayleigh scattering attitude sensor, in: Proc. SPIE, edited by Huffman, R. E. and Stergis, C. G., vol. 2831, pp. 146–153, International Society for Optics and Photonics, doi:10.1117/12.257207, http://proceedings.spiedigitallibrary.org/proceeding.aspx?articleid=1021815http://spie.org/Publications/Proceedings/Paper/10.1117/12.257207?origin{_}id=x4325{&}start{_}volume{_}number=2800, 1996.

Jaross, G., Bhartia, P. K., Chen, G., Kowitt, M., Haken, M., Chen, Z., Xu, P., Warner, J., and Kelly, T.: OMPS Limb Profiler instrument performance assessment, Journal of Geophysical Research: Atmospheres, 119, 4399–4412, doi:10.1002/2013JD020482, http://doi.wiley.com/10.1002/2013JD020482, 2014.

Livesey, N. J., Van Snyder, W., Read, W. G., and Wagner, P. A.: Retrieval algorithms for the EOS Microwave Limb Sounder (MLS), IEEE Transactions on Geoscience and Remote Sensing, 44, 1144–1155, doi:10.1109/TGRS.2006.872327, 2006.

Livesey, N. J., Read, W. G., Wagner, P. A., Froidevaux, L., Lambert, A., Manney, G. L., Millan-Valle, L. F., Pumphrey, H. C., Santee, M. L., Schwartz, M. J., Wang, S., Fuller, R. A., Jarnot, R. F., Knosp, B. W., and Martinez, E.: Version 4.2x Level 2 data quality and description document., Tech. Rep. JPL D-33509, NASA Jet Propulsion Laboratory, version 4.2x–3.0, 2017.

Llewellyn, E. J., Lloyd, N. D., Degenstein, D. A., Gattinger, R. L., Petalina, S. V., Bourassa, A. E., Wiensz, J. T., Ivanov, E. V., McDade, I. C., Solheim, B. H., McConnell, J. C., Haley, C. S., von Savigny, C., Sioris, C. E., McLinden, C. A., Griffioen, E., Kaminski, J., Evans, W. F. J., Puckrin, E., Strong, K., Wehrle, V., Hum, R. H., Kendall, D. J. W., Matsushita, J., Murtagh, D. P., Brohede, S., Stegman, J., Witt, G., Barnes, G., Payne, W. F., Piche, L., Smith, K., Warshaw, G., Deslauniers, D. L., Marchand, P., Richardson, E. H., King, R. A., Wevers, I., McCreath, W., Kyrölä, E., Oikarinen, L., Leppelmeier, G. W., Auvinen, H., Megle, G., Hauchecorne, A., Lefevre, F., de La Noe, J., Ricaud, P., Frisk, U., Sjoberg, F., von Scheele, F., and Nordh, L.: The OSIRIS instrument on the Odin spacecraft, Canadian Journal of Physics, 82:6, s. 4, 411–422, 2004.

Loughman, R. P., Flittner, D. E., Herman, B. M., Bhartia, P. K., Hilsenrath, E., and McPeters, R. D.: Description and sensitivity analysis of a limb scattering ozone retrieval algorithm, Journal of Geophysical Research, 110, D19 301, doi:10.1029/2004JD005429, http://doi.wiley.com/10.1029/2004JD005429, 2005.

Malicet, J., Daumont, D., Charbonnier, J., Parisse, C., Chakir, A., and Brion, J.: Ozone UV spectroscopy. II. Absorption cross-sections and temperature dependence, Journal of atmospheric chemistry, 21, 263–273, 1995.

McPeters, R., Labow, G., and Johnson, B.: A satellite-derived ozone climatology for balloonsonde estimation of total column ozone, Journal of Geophysical Research: Atmospheres, 102, 8875–8885, 1997.

Moy, L., Bhartia, P. K., Jaross, G., Loughman, R., Kramarova, N., Chen, Z., Taha, G., Chen, G., and Xu, P.: Altitude registration of limb-scattered radiation, Atmospheric Measurement Techniques, 10, 167–178, doi:10.5194/AMT-10-167-2017, http://www.atmos-meas-tech.net/10/167/2017/amt-10-167-2017.html, 2017.

Palmer, K. F. and Williams, D.: Optical constants of sulfuric acid; application to the clouds of Venus?, Applied Optics, 14, 208–219, 1975.

Puķīte, J., Kühl, S., Deutschmann, T., Platt, U., and Wagner, T.: Accounting for the effect of horizontal gradients in limb measurements of scattered sunlight, Atmos. Chem. Phys., 8, 3045–3060, doi:10.5194/acp-8-3045-2008, http://www.atmos-chem-phys.net/8/3045/2008/, 2008.

Rault, D. F.: Ozone profile retrieval from Stratospheric Aerosol and Gas Experiment (SAGE III) limb scatter measurements, Journal of Geophysical Research, 110, D09 309, doi:10.1029/2004JD004970, http://doi.wiley.com/10.1029/2004JD004970, 2005.

Rault, D. F. and Loughman, R. P.: The OMPS Limb Profiler Environmental Data Record Algorithm Theoretical Basis Document and Expected Performance, IEEE Transactions on Geoscience and Remote Sensing, 51, 2505–2527, doi:10.1109/TGRS.2012.2213093, http://ieeexplore.ieee.org/document/6329422/, 2013.

Rault, D. F. and Spurr, R.: The OMPS Limb Profiler instrument: two-dimensional retrieval algorithm, in: Remote Sensing, pp. 78 270P—-78 270P, International Society for Optics and Photonics, 2010.

Rodgers, C. D.: Inverse methods for atmospheric sounding: theory and practice, vol. 2, World scientific, 2000.

Sofieva, V. F., Rahpoe, N., Tamminen, J., Kyrölä, E., Kalakoski, N., Weber, M., Rozanov, A., Von Savigny, C., Laeng, A., Von Clarmann, T., Stiller, G., Lossow, S., Degenstein, D., Bourassa, A., Adams, C., Roth, C., Lloyd, N., Bernath, P., Hargreaves, R. J., Urban, J., Murtagh, D., Hauchecorne, A., Dalaudier, F., Van Roozendael, M., Kalb, N., and Zehner, C.: Harmonized dataset of ozone profiles from satellite limb and occultation measurements, Earth System Science Data, 5, 349–363, doi:10.5194/essd-5-349-2013, www.earth-syst-sci-data.net/5/349/2013/http://www.esa-ozone-cci.org/?q=node/161, 2013.

Tikhonov, A. N.: On the stability of inverse problems, in: Dokl. Akad. Nauk SSSR, vol. 39, pp. 195–198, 1943.

von Clarmann, T., De Clercq, C., Ridolfi, M., Höpfner, M., and Lambert, J.-C.: The horizontal resolution of MIPAS, Atmos. Meas. Tech. Discuss., 1, 103–125, doi:10.5194/amtd-1-103-2008, http://www.atmos-meas-tech.net/2/47/2009/, 2008.

von Savigny, C., Haley, C. S., Sioris, C. E., McDade, I. C., Llewellyn, E. J., Degenstein, D., Evans, W. F. J., Gattinger, R. L., Griffioen, E., Kyrölä, E., Lloyd, N. D., McConnell, J. C., McLinden, C. A., Mégie, G., Murtagh, D. P., Solheim, B., and Strong, K.: Stratospheric ozone profiles retrieved from limb scattered sunlight radiance spectra measured by the OSIRIS instrument on the Odin satellite, Geophysical Research Letters, 30, 1755, doi:10.1029/2002GL016401, 2003.

Waters, J. W., Froidevaux, L., Harwood, R. S., Jarnot, R. F., Pickett, H. M., Read, W. G., Siegel, P. H., Cofield, R. E., Filipiak, M. J., Flower, D. A., Holden, J. R., Lau, G. K., Livesey, N. J., Manney, G. L., Pumphrey, H. C., Santee, M. L., Wu, D. L., Cuddy, D. T., Lay, R. R., Loo, M. S., Perun, V. S., Schwartz, M. J., Stek, P. C., Thurstans, R. P., Boyles, M. A., Chandra, K. M., Chavez, M. C., Chen, G. S., Chudasama, B. V., Dodge, R., Fuller, R. A., Girard, M. A., Jiang, J. H., Jiang, Y., Knosp, B. W., Labelle, R. C., Lam, J. C., Lee, K. A., Miller, D., Oswald, J. E., Patel, N. C., Pukala, D. M., Quintero, O., Scaff, D. M., Van Snyder, W., Tope, M. C., Wagner, P. A., and Walch, M. J.: The Earth Observing System Microwave Limb Sounder (EOS MLS) on the aura satellite, IEEE Transactions on Geoscience and Remote Sensing, 44, 1075–1092, doi:10.1109/TGRS.2006.873771, 2006.

Wiscombe, W. J.: Improved Mie scattering algorithms., Applied optics, 19, 1505–9, 1980.

Zawada, D., Bourassa, A., and Degenstein, D.: Two-Dimensional Analytic Weighting Functions For Limb Scattering, Journal of Quantitative Spectroscopy and Radiative Transfer, 200, 125–136, doi:10.1016/j.jqsrt.2017.06.008, http://www.sciencedirect.com/science/article/pii/S0022407317300158, 2017.

Zawada, D. J., Dueck, S. R., Rieger, L. A., Bourassa, A. E., Lloyd, N. D., and Degenstein, D. A.: High-resolution and Monte Carlo additions to the SASKTRAN radiative transfer model, Atmospheric Measurement Techniques, 8, 2609–2623, doi:10.5194/amt-8-2609-2015, 2015.